Performance Analysis of High Contrast Sub Wavelength Grating for Biomedical Sensing Applications

A Thesis

submitted in partial fulfillment of the requirements for the award of the degree of

Doctor of Philosophy

Submitted by

Pallavi Sharma

(Reg no: 951506002)

under the supervision of

Dr. Rajinder Singh Kaler
Senior Professor

Dr. Pradeep Kumar Teotia
Sub Divisional Engineer

Electronics and Communication Engineering Department

Thapar Institute of Engineering and Technology, Patiala, Punjab (India)

(Declared as Deemed-to-be-University u/s 3 of the UGC Act., 1956)

FEB 2025

Candidate Declaration

I hereby certify that the work, which is being presented in the thesis, entitled Performance Analysis of High Contrast Sub Wavelength Grating for Biomedical Sensing Applications, in partial fulfillment of the requirements for the award of the degree of Doctor of Philosophy in Electronics and Communication Engineering from Thapar University, Patiala is an authentic record of my work carried out during the period Jan 2016 to Feb 2025 under the supervision of Dr. R.S. Kaler and Co-Supervisor Pradeep Kumar Teotia. I have also cited the reference about the text(s)/figure(s)/table(s) from where they have been taken.

The matter presented in this thesis has not been submitted elsewhere for the award of any other degree or diploma from any institution.

Date: 28-02-2025

Pallavi Sharma

Candidate

This is to certify that the above statement made by the candidate is correct to the best of our knowledge.

Dr. R. S Kaler

Senior Professor

Supervisor

Dr. Pardeep Kumar Teotia

Sub Divisional Engineer

Co-Supervisor

.....dedicated to my ***Krishan ji, Papa, Mamma, Husband, and My Son Tanish***

ABSTRACT

Traditional biosensing technologies have limitations such as complex sample preparation, expensive operating systems, and limited sensitivity. These constraints have driven the need for advanced sensing platforms with improved performance metrics. Recently, high-contrast subwavelength gratings (HCGs) and surface plasmon resonance have been suggested among the most powerful candidates in optical biosensing since they can manipulate light at a subwavelength scale with a high degree of freedom. Optical biosensors based on HCGs represent a rising class of optical sensors that allow label-free detection non-invasive diagnostics, and in situ place data acquisition, thus providing large advantages over conventional sensing technologies.

High contrast subwavelength gratings (HCSGs) are periodic microstructures with a grating period smaller than the wavelength of incident light. These microstructures exploit resonant effects and photonic band gaps, which permit powerful light-material interactions required for sensitive detection mechanisms. Using these properties, HCGs can work as a promising platform for biosensing applications and eliminate the need for sophisticated approaches. In this research, a performance analytical study of high-contrast subwavelength gratings for biomedical sensing applications has been done and the goal is to improve our design and enlarge their utility in the detection of biomolecular interactions. A generic framework is developed to evaluate the performance of HCSG-based sensors, considering factors such as grating parameters (grating thickness, grating height, grating periods, etc.), the refractive index contrast, and functionality for biomolecular recognition. This research explores the optimization of HCSG-based biosensors, specifically focusing on their design parameters that affect performance metrics such as resolution, sensitivity, and detection limits.

By using advanced simulation techniques, including FDTD (finite-difference time-domain) methods, the study analyses the various effects of design parameters of HCSGs, such as grating period, depth, and duty cycle, on the sensor's sensitivity and performance. Furthermore, parametric research is carried out to establish the most efficient grating design for maximizing sensor performance in real-world biomedical sensing applications.

Highly reflective mirror technologies are majorly required in bio-sensing applications to eliminate complex multiple diffraction orders. Various grating parameters, i.e. width, thickness, and period are analyzed to get optimized values and high reflectivity for high-contrast subwavelength grating (HCSG) structure. Besides these parameters, polarization modes, angle of incidence, and refractive index have been diversely analyzed to monitor their effects on HCSG structure concerning reflectivity. The simulation results manifest that the optimized parameters help to achieve the best reflectivity that can be further utilized in bio-sensing applications. The best-optimized parameters in our research for HCSG structure are polarization mode (TM mode), angle of incidence (0° , 4°), grating width (S = 0.5855 μ m), grating thickness (tg = 0.495 μ m), and grating period (L = 0.77 μ m). Along with these parameters, as the refractive index of the surrounding material of grating changes, a wavelength of reflectivity dip shifts towards the right side. All these parameters result in 99.998% reflectivity for HCSG structure that can be further utilized in bio-sensing applications.

This research's fundamental contribution is the establishment of a structure that considers HCGs' unique properties. The framework includes a set of performance parameters, such as detection limit, sensitivity, and figure of merit, which provide a comprehensive analysis of sensor performance. This evaluation method provides essential facts about how HCGs can be adapted for various medicinal applications and establishes the basis for future research. A high contrast grating-based surface Plasmon resonance-based biosensor with high detection accuracy has been proposed. High sensitivity has been obtained by using a high value of dielectric material. The detection accuracy and sensitivity are optimized utilizing the metal layer thickness and its width in the continuation of periodic gratings. With the help of the finite difference time domain (FDTD), the enhanced values of sensitivity are obtained and compared to the photonic crystal waveguide and surface plasmon resonance sensor. The proposed sensor also overlaps the fabrication constraints of various metals as a high value of dielectric material has been employed. HCG-based plasmonic (SPP) biosensors using Titanium oxide and Indium Tin Oxide (ITO) have been investigated to meet the best configuration. that overlap the fabrication constraints by using a high value of dielectric materials. In comparison to the Photonic crystal waveguide and surface plasmon resonance sensor, the reported sensor exhibits a higher resolution in terms of detection accuracy. The presence of high contrast grating provides stability and improves the

detection accuracy 560 μm^{-1} and sensitivity 3150 nm-RIU^{-1}. The value of a high dielectric constant enhances the interaction of surface plasmon resonance and has the lowest influence on sensitivity DA and S_n. A high value of dielectric constant and periodic grating provides a possibility for this geometry to be acknowledged in any wavelength spectral domain. The research suggests that HCG-based sensors present a feasible path toward highly sensitive, dependable, and compact biosensing devices, especially when paired with plasmonic changes.

LIST OF PUBLICATIONS

International Journal

1. Pallavi Sharma, R S Kaler, P Teotia, *"*Optimization of performance parameters of high-contrast subwavelength grating with high reflectivity for bio-sensing applications*"*, *Optica Applicata*, vol 54, issue 1, pages 115-122, 2024.

I.F.=0.6

2. Pallavi Sharma, Pradeep Kumar Teotia, R S Kaler, *"*Analysis of High Contrast Grating Biosensor using Surface Plasmon Resonance for Enhanced sensitivity and Detection Accuracy*"*, *Optoelectronics and Advanced Materials - Rapid Communications*, vol.19, p.10-16, January-February 2025.

I.F.=0.5

ACKNOWLEDGEMENTS

First and foremost, I would like to pay regard to the **Lord Krishan** for His divine blessings, guidance, and strength throughout this journey. His grace has been my greatest source of inspiration, giving me the perseverance and wisdom to overcome challenges and accomplish this work. All this would not have been possible without the constant support, encouragement, and blessings of my beloved **Papa and Mamma**.

I am profoundly grateful to my **supervisor, Dr. R.S Kaler**, for their invaluable guidance, continuous support, and encouragement throughout my research. Their insightful feedback and expertise have played a crucial role in shaping this work. My sincere thanks also go to my **Co-supervisor, Dr. Pradeep Kumar Teotia**, whose valuable suggestions and mentorship have significantly contributed to the success of this thesis.

I extend my heartfelt appreciation to **Head of the Department, Dr. Kulbir Singh**, for providing me with the necessary resources and a conducive research environment to carry out my work efficiently.

A special note of thanks to **Dr. Harpreet Kaur**, whose discussions, support, and motivation have been instrumental in keeping me inspired.

I would like to thank **Dr. Ankush Kansal** Principal (TPC, Patiala), my **friends, and all my TPC colleagues** for their unwavering support and encouragement. Their motivation and understanding have been instrumental in helping me balance my professional and academic commitments. I am truly grateful for their kindness and cooperation throughout this journey.

Most importantly, I would like to express my sincere and deep gratitude to my parents and family for their love, encouragement, care, and support. Finally, I would like to give a large thanks to my husband, **Mr. Karun Sharma**, for having faith in me and supporting me at every step. Without their support, I would not have completed my Ph.D. program. Finally, I would like to give a lot of love to my son **Tanish Sharma**.

I would also like to thank them for their support and love.

Pallavi Sharma

TABLE OF CONTENTS

LIST OF FIGURES

LIST OF TABLES

LIST OF NOTATIONS

α	Attenuation Constant
Ag	Silver
Al	Aluminium
Au	Gold
β	Propagation Constant
Λ	Grating Period
ϱ_m	Permittivity of metal
ϱ_d	Permittivity of dielectric
μ	Permeability
ω	Angular frequency of the electromagnetic wave
λ_{Bragg}	Bragg Wavelength
n_{eff}	Effective Refractive index
$\in_{\boldsymbol{p}}$	Relative permittivity of the material in which the wave is propagating.
m	Diffraction order
G	Grating vector.
β^{SP}	Surface Plasmon Propagation constant
S_n	Sensitivity

LIST OF ABBREVIATIONS

AOTF	Acoustic Optical Tunable Filter
APM	Argument Principle Method
ATR	Attenuated Total Reflection
CEA	Carcinoembryonic Antigen
DA	Detection Accuracy
DBR	Distributed Bragg Reflector
DDM	Double Dip Method
EGFR	Epidermal Growth Receptor
FDTD	Finite Difference Finite Domain
FWHM	Full Width at Half Maximum
LSP	Localized surface Plasmon
NA	Numerical Aperture
POC	Point of Care
PA	Protective Antigen
RI	Refractive Index
RIU	Refractive Index Unit
SNR	Signal to Noise Ratio
SOI	Silicon on Insulator
SPP	Surface Plasmon Polariton
SPR	Surface Plasmon Resonance
TIR	Total Internal Reflection
TE	Transverse Electric
TM	Transverse Magnetic
VCSEL	Vertical Cavity Surface Emission Laser

CHAPTER 1

INTRODUCTION

1.1 Introduction and Motivation

Over the past three decades, research and development of all optical components have changed due to the growing requirement for quick and reliable data processing and detection methods. As a result, numerous new optical sensing devices that use electromagnetic radiation to detect and process measurements have been developed. Furthermore, advancements in material technology and fabrication techniques have compelled the development of gadgets with intricate structural elements.

Optical components are essential in sensors as they facilitate signal generation and detection, enabling the measurement of light signals that reflect interactions between the sensor and target analytes. These components enhance sensitivity by utilizing elements like waveguides and resonators, which confine light and increase interaction with analytes, allowing for detecting low concentrations. They also enable the evanescent field, improving performance without complex sample preparation, and support real-time monitoring, which is crucial for clinical diagnostics and environmental monitoring applications. Optical components' versatility allows for designing various sensor types for specific applications. Furthermore, advances in optical technology facilitate the miniaturization of sensors, making them portable and user-friendly. There are several applications for biosensors in environmental monitoring, food safety, healthcare, and more.

1.2 Biosensors: An Introduction

Biosensors are considered analytical devices that can investigate the presence of biological or chemical species [1]. They can be used to detect the modification in the internal concentrations of endogenous species as a function of a corporal change induced internally or by the intrusion of a bacterium. Traditional sensing techniques often require resources, significant time, and sometimes invasive methods that are not desirable for routine screening. However, Biosensors, offer many advantages that combat these limitations: Non-invasive and Real-time Monitoring, High Specificity,

Sensitivity and Cost-Effectiveness, Portability and Convenience and Diversity in Applications.

The utilization of biosensors is the latest trend to investigate bacteria, viruses and toxins because of the risks posed by biological and chemical agents.

Thus, Biosensors have wide range of applications:

- Environmental monitoring
- Clinical diagnostics
- Food quality control
- Drug development

Typically, a biosensor uses a biological recognition element that observes the existence of the species under investigation and produces a chemical or physical response that is transformed into a signal through a transducer. The general functioning of a biosensor system is represented in Figure 1.1

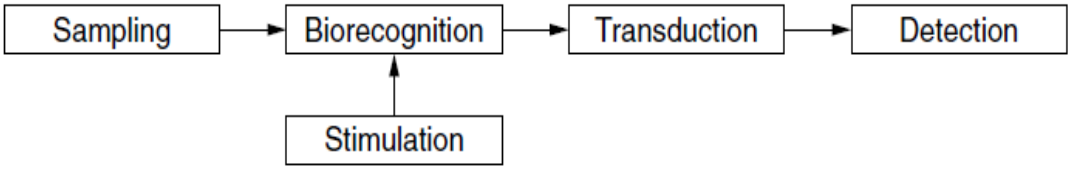

Figure 1.1: General Method of Biosensing [1]

The recognition element binds with a particular analyte the sample unit delivers into the detector to ensure bio-detection specificity. Bio-detection specificity is achieved by the recognition element binding with a specific analyte supplied by the sample unit into the detector. Bio-recognition elements have included antibodies, enzymes, and even organisms such as bacteria or yeast. Biosensors can be categorized into various categories based on signal transduction. Figure 1.2 illustrates optical, magnetic, electrochemical, piezoelectric, or thermometric.

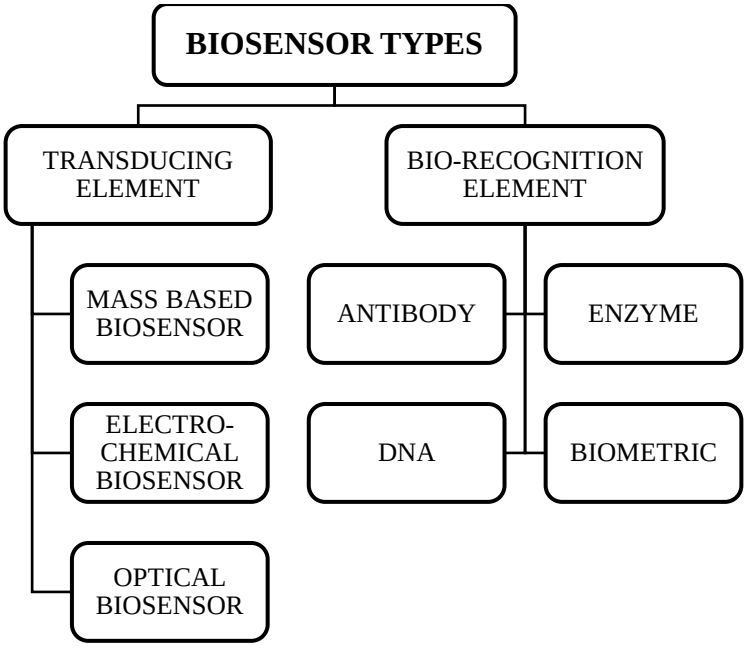

Figure 1.2: Types of Biosensors

The most reported type of biosensor is optical. When the biorecognition element interacts with the optical field. Optical detection is noticed. Usually, electric, optical, or other force fields can be used as stimulation to retrieve a biorecognition result. The transduction process transforms a chemical or physical reaction into an optical or electrical one when stimulation is present. The electrical or optical signal is subsequently detected by the detector device.

Typically, in optical biosensors, the optical input is used in the stimulation process. The transduction process alters the optical signal's amplitude, frequency, phase, or polarization due to physical or chemical changes.

Optical biosensors offer many advantages:

- Remote sensing
- Fast, real-time measurements, Compact Design
- Selectivity and specificity
- Protection against electromagnetic interference
- Detection of several channels and characteristics
- Detailed chemical information on analytes.
- Minimally intrusive for in vivo measurements

Therefore, the key components of optical biosensors are an optical light source, an optical channel (waveguide, fibre, etc.), a fixed biological recognition element (proteins, antibodies, enzymes, etc.), optical transduction (SPR, interferometers, grating, resonators, etc.), and an optical detection method.

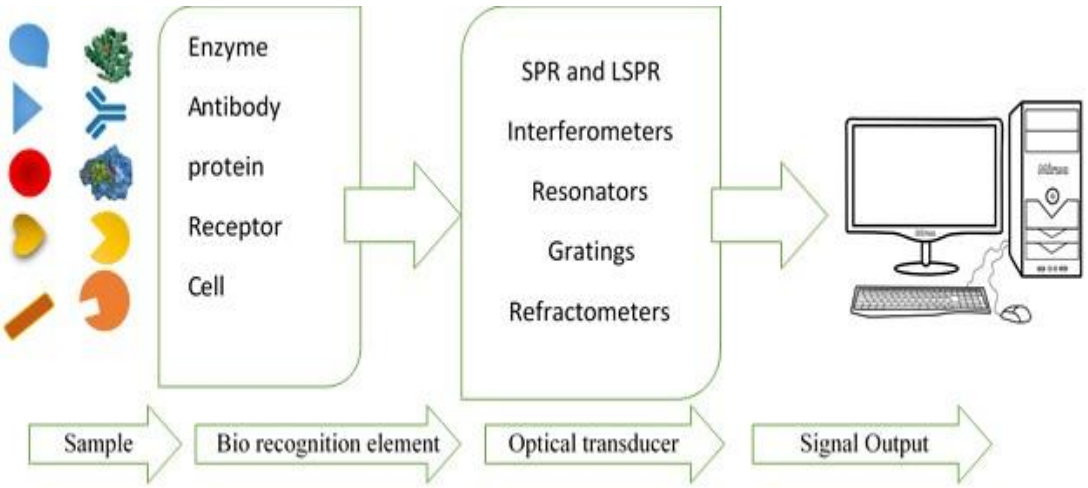

Figure 1.3: Schematic of Optical Biosensors [3]

Label-free and label-based are the two basic categories into which optical biosensing may be divided. In label-free sensing, the transducer's interaction with the material immediately develops the optical signal that must be detected. Label-based sensing, on the other hand, creates the optical signal when the label is added using a fluorescent colorimetric or luminous approach.[3]. Different kinds of optical biosensors [4] exist, including:

1.2.1 Surface Plasmon Resonance Optical Biosensors:

The SPR i.e. Surface Plasmon Resonance event takes place on the surface of conducting substances or metal at the edge of two media when it is illuminated with the specific angle of the polarized light. At the resonance angle, the strength of reflected light decreases because of the development of surface Plasmons. The accumulation on the surface is commensurate to that outcome. By tracking changes in angle, wavelength, or reflectivity over time, the sensitivity could be achieved. A practical SPR apparatus consists of an optical detector element that typically detects changes in intensity, a gold-surfaced sensor chip, and a layer that facilitates ligand immobilization. A fluidics system is also added to enable a flow-through operation. Several applications of SPR

are concentration analysis in numerous fields: clinical, food, environmental investigation, etc.

1.2.2 Localised Surface Plasmon Resonance Optical Biosensor:

A localized surface Plasmon (LSP) is the consequence of the confinement in surface Plasmon in a nanoparticle of size smaller than the light wavelength used to stimulate the plasmon [5]. The LSP has two significant effects: at Plasmon resonant frequency, the optical particle's absorption is maximum and electric fields close to the particle's surface are greatly improved. For nano particles, the maximum optical absorption is occurred in the near-infrared and mid-infrared region. LSPR can be used for nano scale sensing applications, Toxin detection, Identification of cancer biomarkers and DNA hybridization Antigen-antibody interaction screening [6].

1.2.3 Waveguide Interferometric Optical Sensor

Phase difference measurement and evanescent field sensing techniques are used to create a waveguide interferometric optical sensor [7]. When an evanescent field is used to investigate the region in sensor called near-surface, only a little change in the refractive index of the volume being examined results in a guided mode phase shift that corresponds to the reference area. The interference signal generated by these modes' interfering fields is picked up at the sensor's output. The change in the signal is proportional to the refractive index shift and associated with the analyte concentration. Resonant waveguide grating, or RWG, is another name for this technique, which is useful for analysing cellular reactions and functions as well as determining the redistribution of cellular contents [8].

1.2.4 Evanescent Wave Fluorescence Optical Biosensors

In evanescent wave optical biosensors, the consequent binding and the biological recognition event take place within the restrictions of an evanescent wave. Guided light is based on the principle of totally internal reflection; consequently, an evanescent wave arises from the interface of the surrounding and waveguide surface. The evanescent wave declines exponentially with an increase in distance. Only molecules that are fluorescent present near the shallow are activated by sensing that uses an evanescent signal for the excitation work to generate the fluorescent signal. Based on this idea,

numerous biosensors were created, with a broad range of uses spanning from food testing to clinical diagnostics to biodefense [9].

1.2.5 Surface-enhanced Raman scattering biosensors (SERS):

When a molecule is very close to micro metallic surfaces made of gold or silver, a biosensing technique called surface-based Raman scattering (SERS) can increase the concentration of its vibration spectrum by several orders of magnitude. A surface fabricated active in the front of the optical fibres [10] is applied to the sensitive detection of proteins in the low sample volume [11].

A wide range of analytes, including poisons, tumor cells, tumor biomarkers, medications, antibodies, and viruses, can be detected with high sensitivity and selectivity using optical biosensors. Optical biosensors offer sensitive screening of several samples for multiple different parameters on a large scale with high throughput, in addition to offering innovative analytical tools with reduced dimensions [12]. The optical detection method offers a variety of possible in situ detection applications, including remote areas or customized care.

1.3 High Contrast Subwavelength Grating

The many applications of optical diffraction gratings in spectroscopy, lasers, and various optoelectronic devices make them crucial for the subject of study. The two primary regimes of optical gratings are well-inferred: They are widely known in the following regimes: first is a deep subwavelength regime, here gets the grating period less than the incident optical wavelength "λ", and the diffraction area, that have the grating period is bigger than λ [13]. The third zone, i.e. Subwavelength regime, is found to have the period grating lying in between the wavelengths of the grating material and the surrounding media. Except the zeroth order mode, all higher-order diffraction modes are evanescent in this domain. Gratings react completely differently and display distinct characteristics in regions.

1.3.1 Principle of High Contrast Grating

High Index sub-wavelength contrast grating is referred to as a near-wavelength grating construction where low index material completely encloses the high-index grating [14] offered high reflectivity and broadband reflector and demonstrated experimentally [15]

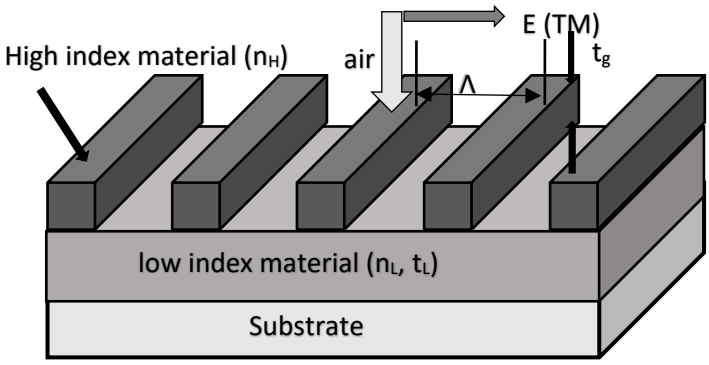

Figure 1.4: Schematic of high contrast grating as broadband reflector [14]

The schematic diagram of high contrast reflectors, which function in the near subwavelength regime and are composed of two low index layers encircling high-index material, is depicted in Figure 1.4. The reflection band is broader when the variance among the low and high indexes is large. The mirror effect depends on the low index layer beneath the grating. High index of refraction materials, low refractive index layer thickness beneath the grating (tl), grating thickness (tg), fill factor, and grating period (Λ) are examples of design factors. The fill factor is the ratio of the grating period to the grating material index's broadness.

One way to think about the HCG grating slabs is as a periodic waveguides array that run along the x axis. Depending on the grating's size and wavelength, certain waveguide modes are excited when a plane wave strikes it [16]. There is a wide range of wavelengths with only two modes that convey energy and have propagation constants in the z direction because of the high index contrast. The regime of interest is this one. After leaving the input plane (z = .0), these two modes go in a downward direction (+z direction) to the grating output plane (z = tg) before reflecting upward. The evanescent waves are the shape of the higher-order modes.

As each mode travels through the HCG thickness tg, it gains a distinct phase. At the HCG output, the reflection of the propagating waveguide modes occurs along with pairing of each other. By one round trip of modes, the reflectivity solution arrives. It should be mentioned that at the input and departure planes, the modes are also transmitted to low-index medium. i.e. air.

However, only the zeroth diffraction order, which is plane waves, carries energy in reflection and transmission because of HCG's subwavelength period in air. This is

arguably one of HCG's most significant characteristics. One of the crucial design factors that regulate their interference and look at the phase that the modes reach is the HCG thickness. [17].

The HCG thickness for high reflection should be selected in a way that causes destructive interference at the exit plane, cancelling transmission. However, to achieve full transmission [18], the thickness should be selected so that the interference equals the input plane wave at the input plane. Constructive interference at the input and exit planes can assist create a high Q resonator.

1.3.2 Features of High Contrast (HC) Sub-Wavelength Grating

The grouping of low-index and high materials provided remarkable unanticipated properties. HCG has a lot of benefits. [19]:

- It provides high reflectivity (>98.5%) broadband spectrum ($\Delta\lambda/\lambda$>30%) with surface normal incident light.
- It enables high polarization stability.
- With the use of HCG in VCSEL stable high single-mode output power is attained.
- Wafer bonding of upper mirror DBRs in the manufacturing process of long wavelength VCSELs is averted.
- HCG facilitates an efficient tuneable VCSEL due to its lightweight with 1/1000-times lesser power consumption and 30-times faster-tuning speed than the traditional tuneable VCSEL based on DBR.
- It offers High-Quality factor Resonance which is of vast importance in several areas like filters, and laser sensors

1.3.3 Applications of High Contrast subwavelength grating

There are numerous beneficial application areas of the near-wavelength HC Gratings

1. *High contrast grating as a Reflecting mirror in a VCSEL*

A VCSEL generates optical light by sandwiching two thick Distributed Bragg Reflecting mirrors between a brief active zone, or cavity. A DBR is a layer of materials with varying refractive indices. Because of the VCSEL's small cavity length, very high reflectivity (>99.5%) is needed to laser light in the VCSEL. However, the resources

employed in DBR assemblies frequently have slight variations in refractive index due to issues in epitaxial growth for attaining alike lattice constants.

In many material systems, epitaxial issues arise because large reflectivity needs a significant number of DBR pairs—typically pairs should be 25–40.

This difficulty is the main barrier to developing VCSELs in a range of wavelength regimes, such as mid-infrared and green-blue. HCGs are a great alternative to DBR mirrors in DBR-based optical devices, such as VCSELs. Higher order transverse mode suppression, stable and controllable output polarization, and exceptionally high tolerance to fabrication error are just a few of the ways that an HCG-based top reflector VCSEL enhances VCSEL performance in addition to providing sufficient optical feedback to enable VCSEL lasing [20].

High-contrast grating-incorporated VCSELs have a considerable fabrication tolerance, which makes them appropriate for WDM applications and low-cost manufacturing [21]. Nowadays, HCGs are used in VCSELs to replace the traditional distributed Bragg reflectors (DBRs) throughout a wide wavelength range of 850 to 1550 nm.

2. High Contrast grating as a Tuneable VCSEL

Earlier MEMS-VCSELs were increased with the thickness of DBR, making them relatively large, usually ∼10–20 μm broad and 200 μm long [22]. This leads to slow processing challenges and tuning speed. Using very thin HCGs i.e. 10–20 times thinner than a normal DBR, the additional proportions of Micro-Electro-Mechanical Systems (MEMS) are decreased by comparable magnitudes, increasing tuning speed. Bottom n-doped DBR, active area, AlGa As oxidation layer top p-doped DBR two pairs, sacrificial layer, and top mirror n-doped HCG are all monolithically produced on a GaAs substrate in the novel tuneable VCSEL design that incorporates HCG.

Over an unidentified air gap, the HCG is freely attached and maintained by a structure with nano-mechanical properties [23]. A typical adjustable VCSEL integrating TM-HCG has a comparatively 200 μA threshold current and 0.25 mW mA^(-1) of slope efficiency. Due to a phase mismatch between the VCSEL and HCG cavities, a gap is observed between 6 and 9 V. This gap can be discarded with a rectified air gap [24]**.** A strong mechanical tuning response of more than 27 MHz is obtained by shrinking the size of HCG and mixing it on a VCSEL with wavelength tunability. Compared to

the previously published adjustable VCSELs, this offers a significant improvement [25,26].

3. HCG VCSEL multi-wavelength array

Multi-wavelength integrated VCSEL arrays are made monolithically via DBR layer thickness changes, which are difficult procedures that are difficult to scale to large arrays [27]. The broadband mirror example illustrates how the reflection spectrum of an HCG can be configured for significant dependency on a lithographically-dependent emission VCSEL wavelength, or, on the other hand, to have an almost negligible wavelength dependence. The same HCG and identical cavity layer thicknesses must be maintained to obtain a large VCSEL wavelength range using the same epitaxy. This requires designing an HCG whose phase can be greatly adjusted by varying the duty cycle and grating period.

Destructive interference takes place in the thick structure of HCG, allowing the waveguide array modes to propagate over a longer length. This results in a high reflectivity with a stronger wavelength dependency in phase.

4. Surface normal emitting High Q Resonator using HCG

Surface normal emission-based high-quality (Q) factor optical resonators have drawn a lot of interest for a range of uses, such as optical sensors, filters, and single photon sources. High-Q resonators have been created using a variety of designs, including distributed Bragg reflectors (DBRs), photonic crystals, ring resonators, and microdisks. While this configuration makes it easier to integrate devices in a cascaded manner, it does not allow for easy connection with fiber or free-space optics. [28]

By altering the periods of high contrast grating placed between DBR grating, the quality factor can be shifted to igh or low. By increasing 3, 5, 7, and 15 periods of HCG placed between DBR grating, the Quality factor is observed to be 900, 4000, 17000, and 500,000 respectively.

5. High Contrast grating as Low Loss Hollow Core Waveguide

Since the core material is eliminated, hollow waveguides can attain fiber-like ultralow loss, dispersion, and nonlinearity. HWs have been handled in a variety of ways, including waveguides with a metallic shell, DBRs, PhCs, etc. The basic idea is to use repeated reflections from cladding reflecting mirrors to guide the optical beam as it

travels through the waveguide. The minimal loss for chip-based HW in a DBR waveguide is more than 10 dB/m, but the minimum loss in a hollow-core PhC optical fiber is 0.001 dB/m. The primary cause of the waveguide's loss is the cladding DBR mirrors' insufficient reflectivity [29]. To achieve very low-loss hollow waveguides, high reflectivity is required.

An HCW can be produced by light propagating between two parallel High Contrast Gratings [30]. By altering the phase of the reflection coefficient in a hollow-core waveguide, slow light can be seen [31]. Consequently, it is possible to effectively switch the direction of light propagation from surface-normal to index-guided in-plane waveguide and vice versa [32]. A single HCG layer can build a tiny optical coupler and splitter by entirely isolating two nearby hollow-core waveguides [33].

1.4 Using High Contrast Subwavelength Grating (HCG) for Biomedical Sensing Applications

High Contrast Gratings (HCGs) have gathered attention for potential applications in biomedical sensing because of their high sensitivity, label-free detection, and miniaturization capabilities. HCG characteristics make it suitable for point-of-care devices and advanced diagnostic tools devices [34]. There are a few key motivations for HCG use in biomedical sensing,

1. Improved Sensitivity for Molecular Detection

HCGs have strong resonance effects which leads to increased sensitivity in detecting biomolecules. This property helps in early-stage disease diagnosis, where biomarkers may exist in low concentrations. The HCG sensitivity can facilitate the detection [35] of small amounts of target molecules, providing better disease management and early diagnosis.

2. Miniaturization and Integration with Lab-on-Chip Devices

Miniaturization of HCG fabrication on the micro and nanoscale enables the development of portable, efficient, and compact diagnostic platforms. This makes it possible to include them into lab-on-a-chip (LOC) devices. The downsizing of sensing devices is essential for point-of-care applications, where a variety of clinical scenarios require quick and accurate diagnosis. [36]

3. Enhanced SNR

The HCGs give high SNR (Signal-to-noise ratio) because of their periodic structure enables accurate detection of infections or weak signals, and biomarkers that are recognized in low concentrations are frequently encountered in biomedical sensing applications.

4. Non-Invasive Label-free detection

One of the primary advantages of HCGs is their capability to perform label-free detection, which eliminates the need for complex and time-consuming labelling processes. This feature makes sensors ideal for real-time diagnostics [37].

5. High-Throughput Screening

The high-throughput capabilities make them appropriate for applications of the simultaneous analysis of multiple samples or biomarkers, such as pathogen detection and drug discovery. This multiplexing ability can enhance the efficiency of screening processes in biomedical research.

6. Multiplexed Detection for Complex Diseases

HCGs can be directed to aid the instantaneous detection of multiple biomarkers, which is important for complex disease diagnostics such as cancer. For the analysis of several biomarkers in a single test, Multiplexed detection is used. This will improve diagnostic accuracy and aiding in personalized treatment planning.

1.5 Surface Plasmon Resonance

Surface Plasmon Resonance (SPR) is an influential and multipurpose optical technique based on the phenomenon of the total internal reflection expansively employed for investigating chemical sensing biomolecular interactions [38], and material characterization in real-time applications.

1.5.1 Principle of SPR

It operates based on coherent electron oscillations at the interface between a metal and a dielectric medium, known as surface plasmons. Under certain circumstances, polarized light can excite these surface plasmons at the interface, creating a resonance phenomenon that is sensitive to variations in the refractive index close to the metal surface. [39].

In the typical SPR setup, light is guided through a prism on top of a thin metal film, usually, gold or silver, placed on the prism's base.

Surface plasmons are created when light strikes a tiny layer of metal at a specific angle, called the resonance angle. Electron surface plasmon waves interact with light on the metal's surface. This optical phenomenon is known as surface plasmon resonance (SPR). When this interaction occurs, an electromagnetic wave propagates along the metal-dielectric interface. The longitudinal electric field or p-polarized wave that accompanies these surface plasmons decays exponentially in both metal and dielectric. The field's highest value occurs at the metal-dielectric interface itself because of this exponential reduction in field intensity [41].

There are essentially two kinds of surface plasmons. (a) Surface Plasmons at Long Range [42] (b) Surface Plasmons at Short Range. We have previously investigated the existence of surface plasmons on the metal-dielectric surface. It is thought that coupling between the surface plasmons at both boundaries occurs if the metal layer is thinly layered between two dielectrics.

This interaction causes a manifest drop in the strength of the reflected light. The resonance angle is extremely sensitive to deviations in the refractive index adjacent to the metal film. Consequently, it is possible to quickly identify any chemical interactions on the sensor surface that alter the local refractive index without assigning specific names to the molecules. SPR is a helpful technique for label-free real-time detection of molecule interaction since it is sensitive to changes in the refractive index close to the metal surface [43]. In SPR research, the resonance conditions are satisfied when polarized light is directed onto a thin metal sheet, typically gold (Au). Because the energy of the incident photons is equal to the energy needed to excite the SPs, the intensity of the reflected light diminishes at a specific angle or wavelength [44]. This resonance is strongly affected by changes in the RI of the surrounding medium. The wavelength or resonance angle SPR is a helpful technique for label-free real-time detection of molecule interaction since it is sensitive to changes in the refractive index close to the metal surface. In SPR research, the resonance conditions are satisfied when polarized light is directed onto a thin metal sheet, typically gold (Au). By detecting these shifts, SPR makes it possible to precisely assess biomolecular interactions, such as binding affinities, kinetics, and concentrations. Another noticeable growth is the development of fibre-optic SPR sensors [45]. Because of these characteristics,

nanostructures are extremely beneficial in a variety of domains, such as materials research, biological sensing, photonics, and electronics [46]

The attenuation and propagation constant of antisymmetric surface plasmons decreases with increasing metal layer thickness. As opposed to antisymmetric surface plasmons, symmetric surface plasmons show less attenuation. These surface plasmons are known as long-range surface plasmons because of their decreased attenuation. These surface plasmons are called long-range surface plasmons because of their lower attenuation, while the antisymmetric mode of surface plasmons is called a short-range plasmon [47, 48]. Building upon this concept, essential configurations were presented to develop the core theory of surface plasmon resonance at the metal-dielectric interface.

1.6 Optical Coupling Techniques

1.6.1 Prism Coupling

The attenuated total reflection (ATR) method can be used to excite surface plasmons through a prism coupler. Two primary combinations are frequently used to define this method:

- Otto Configuration: In this configuration, a laser beam is directed at the bottom surface of a coupling prism to couple an evanescent wave to the surface plasmon wave. At the prism-air contact, the incidence angle is marginally larger than the critical angle (θ_{ATR}). The following is an expression for the evanescent wave's propagation constant along this interface [47]:

$$K_s = \left(\frac{\omega}{c}\right)\left(\epsilon_p\right)^{1/2} \sin\ \theta \qquad (1.1)$$

The evanescent field can excite surface plasmons at the air-metal interface if a metal surface is placed near enough to this decaying evanescent field, with an air gap between the metal layer and the prism base shown in Figure 1.5(a). This arrangement is less useful, though, because it is difficult to keep the metal within 200 nm of the prism surface.

- Kretschmann–Raether Configuration: This approach, which is a modification over the Otto configuration, implies directly coating the prism's base with a small layer of metal (approximately 50 nm) shown in Figure 1.5 (b). At an angle $\theta \geq \theta_{ATR}$. p-polarised light incident through the prism produces an evanescent wave at the prism metal contact. The metal dielectric interface's surface

plasmons may be excited by this wave. The following describes the resonance condition [48]:

$$(\frac{\omega}{c})(\epsilon_p)^{\frac{1}{2}}\sin\ \theta_{\text{res}} = (\frac{\omega}{c})\left(\frac{\epsilon_s\epsilon_m}{\epsilon_s+\epsilon_m}\right)^{1/2} \quad (1.2)$$

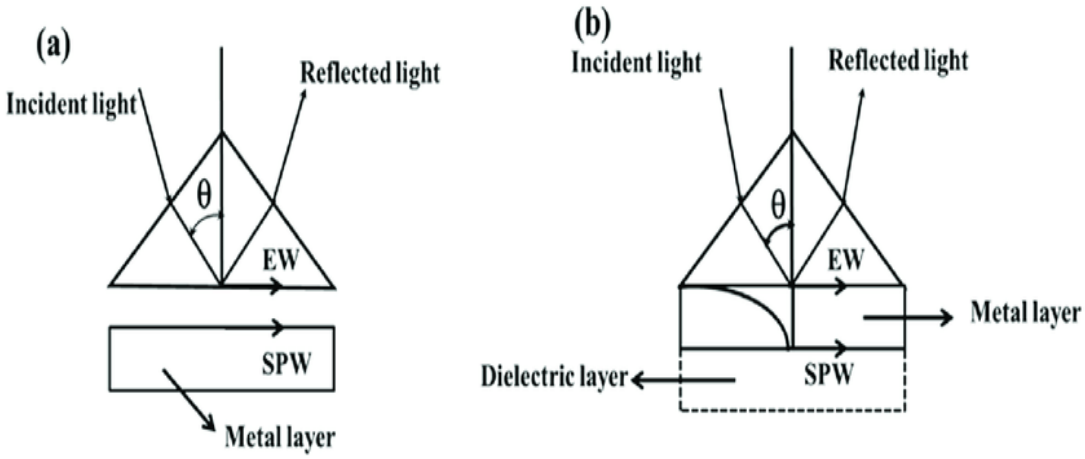

Figure 1.5: (a) Otto Configuration (b) Kretschmann–Raether Configuration of Surface Plasmon Resonance

1.6.2 Grating Coupling

In addition to prism coupling, surface plasmon excitation requires additional techniques. Light diffraction on diffraction gratings is the basis for its operation. In this coupling approach, gratings with grating depth h and grating period Λ are struck by a light wave with wave vector k depicted in Figure 1.6. The wave vector of light diffracted by a periodic grating structure can be expressed as [49].

$$k_m = k + mG \quad (1.3)$$

Where G represents the grating vector and m denotes diffraction order. The wave vector's magnitude is inversely proportional to the grating's pitch and is typically aligned perpendicular to it. It can be expressed as [49]

$$G = \frac{2\pi}{\Lambda} z_0 \quad (1.4)$$

By utilizing wave vector and grating vector equations represented in 1.3 and 1.4, the equation is altered by considering the k_{xm} is the incident wave [49]

$$k_{zm} = k_z + m\frac{2\pi}{\Lambda} \quad (1.5)$$

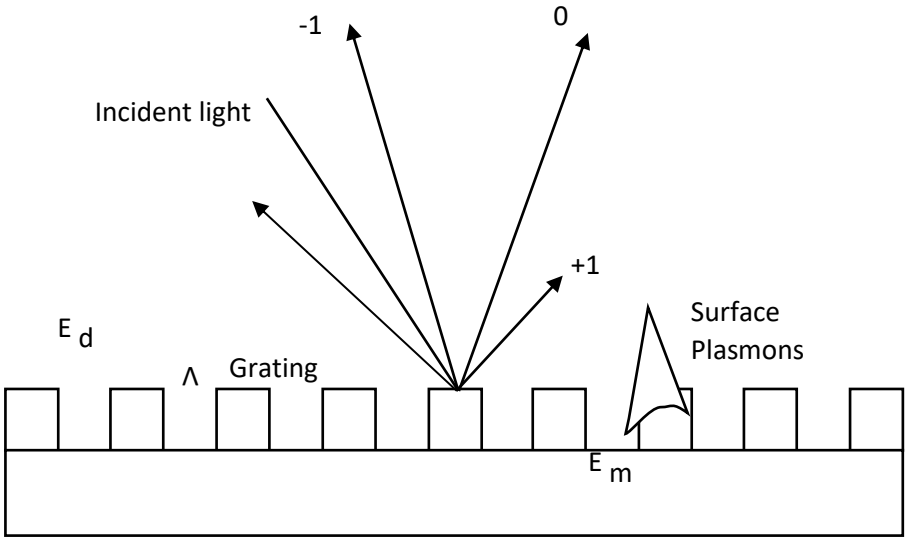

Figure 1.6: Excitation of surface plasmons by grating coupling

whereas β^{SP} can be understood as [49]

$$\beta^{SP} = \beta^{SP_0} + \Delta\beta = \frac{\omega}{c}\left(\frac{\epsilon_s \epsilon_m}{\epsilon_s + \epsilon_m}\right)^{1/2} + \Delta\beta \tag{1.6}$$

where β^{SP_0} is the surface plasmon propagation constant at metal-dielectric interface and $\Delta\beta$ denotes the grating. In terms of effective refractive index, the grating coupling condition can be expressed as [50]

$$n_d \sin\,\theta + m\frac{\lambda}{\Lambda} = \pm\left(Re\left\{\left(\frac{\epsilon_s \epsilon_m}{\epsilon_s + \epsilon_m}\right)^{1/2}\right\} + \Delta n_{eff}^{SP}\right. \tag{1.7}$$

where $\Delta n_{\text{eff}}^{SP} = \text{Re}\left\{\frac{\Delta\beta\lambda}{2\pi}\right\}$.

It can be seen from eq. 1.7 that various different combinations of diffraction order, angle of incidence, and grating pitch have been explored in order to achieve the grating coupling requirement. The primary characteristic of grating coupling is that the reflectance dip is entirely dependent on the grating depth [51]. Nonetheless, there are two additional types of grating coupling: direct and indirect. Whereas indirect grating coupling entails coupling light through a prism or waveguide, direct grating coupling brought incident light from the dielectric side into direct contact with the metal-dielectric interface [52,53].

1.6.3. Waveguide Coupling

It is possible to excite surface plasmons using dielectric waveguide modes. The coupling mechanism between a metal-dielectric waveguide is depicted in Figure 1.7. This technique enables the coupling of surface plasmons at the metal layer's outer boundary by propagating a waveguide mode along the waveguide and into the metal layer region. To achieve optimal coupling, the propagation constant of the waveguide mode must match the surface plasmon propagation constant. The complete equation is given as follows [54].

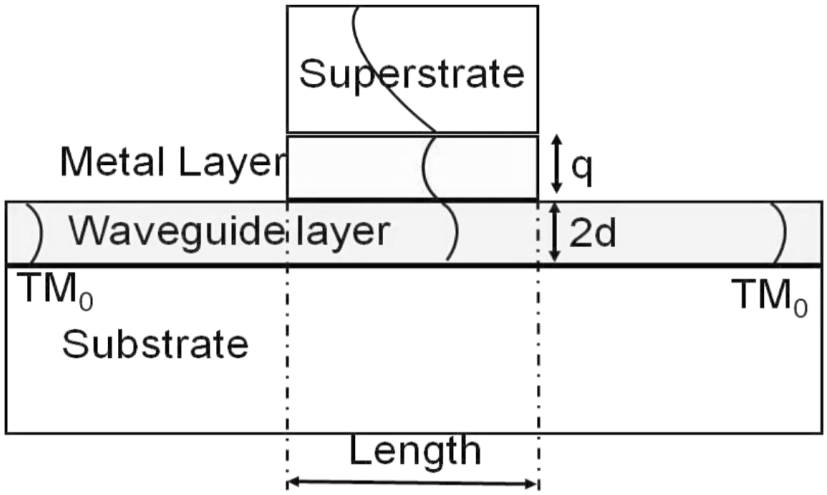

Figure 1.7: Surface plasmons excitation by waveguide mode

$$\beta_{WM} = \mathrm{Re}\{\beta_{SP}\} \tag{1.8}$$

It is also important to note that waveguide modes exhibit lower dispersion compared to surface plasmon modes, as indicated by Equation 1.8

1.7 Features of SPR Sensors

The performance of SPR sensors can be evaluated using the parameters listed below. To achieve optimal performance and improved sensing capabilities, both sensitivity and detection accuracy (signal-to-noise ratio, SNR) should be maximized.

1. Sensitivity

The amount that a small change in the refractive index of an analyte or sensing layer causes a shift in the resonance wavelength is known as the sensor's sensitivity. A significant shift signifies high sensitivity.

When the refractive index raises by a certain amount, the resonance wavelength shifts by an equal amount. The sensitivity of an SPR sensor is defined in the context of the wavelength interrogation method [55].

$$S_n = \frac{\Delta\lambda_{\text{res}}}{\delta n_s} \tag{1.9}$$

2. SNR (Signal to Noise Ratio) or Detection Accuracy

The ability of an SPR sensor to precisely and accurately detect light parameters, such as resonance wavelength and angle, in relation to the analyte's or sensing layer's refractive index is known as the Signal to Noise Ratio (SNR) or detection accuracy.

As the width of the SPR curve becomes narrower, the detection accuracy increases. The resonance wavelength $\Delta\lambda_{\text{res}}$ get shifted with refractive index change of the analyte or sensing layer ns by δns.

Using Wavelength interrogation techniques, the Signal to noise ratio also known as detection accuracy can be calculated with the following equation [47]

$$\text{SNR} = \frac{S_n}{\delta\text{ns}} \tag{1.10}$$

The accuracy of the SPR sensing system's detection or actual signal-to-noise ratio (SNR) is largely dependent on how accurately actual equipment can measure the signal.

3. Quality Factor

The key performance parameter of the sensor based on surface plasmon resonance is the quality Factor also known as the figure of Merit and can be calculated with the help of the following equation [56,57]:

$$Q.F = \frac{S_n}{FWHM} \tag{1.11}$$

To get high-performance sensors, maximum and better sensitivity, and FoM levels are necessary.

1.8. Applications and Advancements of SPR Technology

SPR's use in real-time monitoring and label-free detection capabilities has made it a cornerstone of biosensor advancement. It provides the investigation of binding kinetics and affinity and enables the observation of interactions between different biomolecules,

including proteins, small compounds, and nucleic acids. SPR is used to detect specific DNA sequences, monitor antibody-antigen interactions, and identify biomarkers for diseases. Recent developments have increased the abilities of SPR-based sensors. The integration of nanomaterials, such as graphene and gold nanoparticles, has directed to major enhancements in sensitivity and specificity. Graphene's properties like large surface area and high electrical conductivity facilitate the immobilization of biomolecules, enhancing sensor performance. Furthermore, the incorporation of graphene has been shown to enhance the resistance of SPR sensors to high-temperature annealing, broadening their applicability dispersion wavelength [58] environments.

By integrating SPR on to optical fibres, these sensors offer compactness and the potential for remote sensing applications. This format is particularly valuable in field applications where traditional SPR setups may be impractical.

Nanostructures are minuscule structures that range in size from 1 to 100 nanometres. Because of their large surface-area-to-volume ratios and quantum effects, they have special optical, electrical, mechanical, and chemical properties.

1.9 Conclusion

High Contrast Gratings (HCGs) are attracting attention in biomedical sensing because they are incredibly sensitive, can be made small, and do not require labels to detect things. This makes them ideal for things like real-time health monitoring, rapid tests at the clinic, and even spotting hard-to-diagnose diseases. As technology keeps improving, HCG-based sensors are composed to change the way we diagnose and manage health, offering quicker, more accurate, and accessible solutions for everyone. Despite the significant advancements, challenges remain in the field of SPR sensing. Improving the sensitivity and specificity of SPR sensors continues to be a primary focus. Strategies such as surface modification and the use of advanced nanomaterials are being explored to address these challenges. Additionally, expanding the range of detectable analytes and enhancing the robustness of SPR sensors in various environmental conditions are ongoing areas of research. The integration of SPR with other analytical techniques, such as electrochemistry, is also a promising avenue. This combination can provide complementary information, enhancing the overall analytical capabilities of SPR-based systems.

1.10 Organization of Thesis

There will be five chapters in the thesis. A brief outline is provided here:

Chapter 1: The main introduction and motivation of the research are presented in this chapter. It also discusses theoretical concepts. Additionally, we outline the biosensors, types of biosensors, the need for optical biosensors in the biomedical field, a detailed description of High contrast subwavelength grating, principle of operation, features and several applications in various fields, introduction to surface plasmon resonance, their principle of operation. HCG and Surface plasmon resonance are used in Biomedical sensing applications.

Chapter 2: This chapter consists of a review of the literature and important research gaps are present in this chapter. Additionally, the chapter defines the research aims and methodology used in this study. The thesis outline presented in this chapter

Chapter 3: This chapter describes the impact of gratings and multilayer designs for a variety of applications and examines how different optical characteristics affect the design of the high-contrast subwavelength grating.

Chapter 4: The proposed design, which makes use of several plasmonic metals and dielectrics to improve the sensitivity and detection accuracy for the identification of biological species, is demonstrated in this chapter.

Chapter 5: The main conclusions and contributions of the thesis are summarized in this chapter, along with possible directions for further investigation. The work emphasizes how the use of SPR-based sensors for HCG detection significantly affects commercial sensors by including grating effects and multilayer designs. Through the introduction of the multilayer and grating effect, the current work demonstrates a positive influence of SPR-based sensors on commercial sensors. Additionally, it was discovered that multilayer not only overcomes the shortcomings but also, with an optimal design, satisfies the accuracy and sensitivity requirements. Additionally, it was noted that the presence of various dielectric combinations with metals results in improved wavelength shift, which is highly beneficial for medical diagnosis.

CHAPTER 2

LITERATURE SURVEY

2.1 Introduction

High contrast grating (HCG) structures have drawn a lot of interest due to the development of biosensing technology since they increase the sensitivity of detection. HCG-based biosensors improve performance in biomedical applications by manipulating light-matter interactions through periodic nanostructures. When integrated with surface plasmon resonance (SPR), these structures offer superior optical confinement, leading to increased sensitivity and accuracy in biomolecular detection. Various studies have explored the design, fabrication, and optimization of HCG-SPR biosensors, focusing on factors such as grating period, material selection, and resonance conditions. This literature survey examines recent advancements in HCG biosensors, highlighting key contributions in modelling approaches, experimental validations, and potential applications in biomedical diagnostics.

2.2 Review of High contrast Sub Wavelength Grating: Advancements and applications

C.F.R. Mateus et al.[59] described the design and experimental description of a subwavelength grating with a very broad reflection spectrum under normal incoming light . The outcomes of simulations and experiments are comparable. It is easy to scale the grating's dimensions by multiplying the mirror dimensions by a constant. Its monolithic manufacturing makes it simple to integrate with other optoelectronic devices. This sub wavelength grating reflecting mirror has potential application for many passive and active devices like reconfigurable focal plane arrays, microelectromechanical tuneable devices, and visible and infrared wavelength VCSELs.

S. Chung et al. [60] proposed and quantitatively examined a novel vertical-cavity surface-emitting laser (VCSEL) construction based on a thin oxide gap and a subwavelength grating mirror. As a grating mirror, the structure has demonstrated comparable threshold gain, suppression of higher-order transverse modes, and polarization stability. According to VCSEL, the narrow oxide gap construction has

several benefits, such as enhanced mechanical stability, easy fabrication, and extremely stable single mode characteristics.

The development of a single-layer, one-dimensional, high-index contrast subwavelength grating structure was reviewed by C.J. Chang-Hasnain et al. [61]. Large aperture, single-transverse-mode control, simple fabrication, and lithographically defined polarization control are all made possible by VCSEL with HCG. With a variance of ±20% in the essential dimension of the high-contrast grating (HCG), an exceptionally high fabrication tolerance is established. A 40% variation in the lithography linewidth results in a 0.2% variation in the emission wavelength of HCG-VCSEL. The size of the adjustable reflecting mirror was reduced by 8000 times and the tuning speed was increased by 160 times to 63 ns when tuneable VCSELs were fabricated utilizing HCG. With this setup, a large variety of optoelectronic devices in a wide range of wavelengths will be available.

An electrically pumped high contrast grating (HCG) VCSEL with a proton implant-defined aperture functioning at 1550 nm was demonstrated by C. Chase et al. [62]. At room temperature, output powers greater than 1 mW are obtained during continuous wave operation. At temperatures higher than 60° C, devices run continuously. Long wavelength VCSELs that are less expensive might be made possible by the innovative device design that was created in a single epitaxy operation.

Y. Zhou et al. [63] studied high index-contrast subwavelength gratings (HCGs) and their many uses in optoelectronic devices, such as low-loss hollow-core waveguides (HWs), high-quality optical resonators, tuneable VCSELs, and VCSELs. A novel HCG hollow waveguide design with an ultralow propagation loss of less than 0.01 dB/m and shallow angle reflectors are also discussed. This novel HCG HW can be used as a key component in many applications, such as optical delay lines, optical interconnects, and optical sensors.

W. Yang et al. [64] presented a completely new wave guiding idea utilizing two parallel planar silicon-on-insulator wafers and high-contrast subwavelength gratings to reflect light in between. Gas sensors, laser surgery, and non-linear optics are just a few of the novel uses for hollow-core waveguides (HCWs) based on optical fibre. Chip-scale HCWs have the advantages of being small, light, and able to be integrated with other devices. However, the absence of low loss waveguide design has hindered their

progress. Two-dimensional light confinement is perceived experimentally with no sidewalls in the HCWs, which is capable for ultrafast sensing response with nearly instantaneous flow of gases or fluids. Using created 9-μm waveguide HCW, a single mode Fiber is mode-matched to a low optical loss of 0.37 dB/cm. This novel waveguide design created a whole new method for lab-on-a-chip applications and inexpensive chip-scale sensor arrays.

A. Taghizadeh *et al*. [65] presented a new design of hybrid grating reflector having high reflectivity with wide wavelength range and the structure appropriate for a vertical cavity laser with very small modal volume. The properties of hybrid grating reflectors are numerically investigated and explained. A Si grating and an unpattern III-V layer make up the HG. In comparison to the well-known high-index-contrast grating (HCG), the III-V layer offers more guided mode resonances, has a thickness equal to the grating layer, and significantly expands the reflector's bandwidth.

A. Liu et al. [66] proposed low Q guided modes for finite-size high-contrast gratings (HCGs). A fraction of the finite-size incident wave can be transformed into the in-plane direction using these modes. These finite-size HCGs with guided modes are proposed here for optical sensors with an on-chip integrated p-i-n photodiode on the same HCG layer. The proposed integrated HCG-based optical sensors' performance and guided mode characteristics are investigated. The proposed HCG-based integrated optical sensors are small, label-free, extremely sensitive, and relatively priced. They may be enlarged to an array configuration, which boosts throughput.

Y. Wang et al. [67] reported using a silicon nitride membrane with a thickness of 500 nm as a high reflective mirror in the orange-red spectral band. Semiconductor-based high-contrast gratings have already been employed as high-reflective mirrors in the near-infrared range. But far less focus has been placed on their use in the visible spectrum, which is crucial for many types of biosensors. Our membrane, which is a part of an adjustable Fabry-Perot cavity, was created using a 560 nm-period high contrast grating. The electrostatically adjusted cavity serves as an optical filter. In order to implant the effect of arm geometry on surface stress and membrane displacement, three different membrane suspension designs are investigated. By biasing the device with 9 V, 13-nm wavelength shifts from the spectral peak (centered at 630 nm).

The optical characteristics of two-dimensional (2D) high-contrast gratings were examined by P. Qiao et al. [68], who also examined the methods by which HCG can serve as a range of high-performance optical components. A wide range of applications, including reflectors, filters, 2D phase plates, 2-Dimensional OCDMA resonators, and even wave plates, can be efficiently engineered using the top-down design process. The designed structures' simulation results show very high power efficiency and good compliance with the expected functionality.

A new label-free biosensor based on a high contrast grating resonator using silicon as a high index material with Q~3000 was introduced by T. Sun et al. [69]. It was discovered that the biosensor can detect target proteins with a sensitivity of 100 pg/ml and is simple to connect to a single-mode fiber.

I.S. Chung [70] proposed a theoretical study of differences for TM and TE polarizations in wideband high-index contrast grating (HCG) reflectors, covering several grating properties and parameters of HCGs. It is revealed that the TM-HCG reflectors have smaller grating periods and larger grating thicknesses than the HCG with TE Polarization reflectors. This difference originates from the various boundary conditions for the electric field of both polarizations. Due to this the HCG with TM Polarization reflectors have much smaller evanescent extension of modes into low-refractive-index media enclosing the HCG. It facilitates to attain a very short cavity length for VCSELs, that is important for MEMS-tunable VCSELs and ultrahigh speed VCSELs.

Improved four-wave mixing using a silicon HCG resonator on a silicon-on-insulator (SOI) wafer immediately copulated by a free space Gaussian beam in the surface-normal direction was demonstrated by T. Sun et al. [71]. The HCG resonator has a quality factor of about 7330 and a peak conversion efficiency of about 19.5dB at low pumping power of about 900μW. A stable and simple alignment mechanism is made possible by surface normal coupling. The device's tiny size and excellent efficiency make it an effective way to convert wavelengths in chip-scale integrated optics.

Integrable GaAs high-contrast gratings were presented by A. Liu et al. [72] and are manufactured and characterized to meet the needs of high-speed VCSEL applications. For the transverse magnetic polarization of finite-size HCG, the computed findings accord with the experimental measurements, which indicate a 93% reflectivity (from

1270 to 1330 nm). The GaAs substrate, various air gaps, and HCGs combine to form the Fabry Perot filter array based on HCG.

The simulated result of resonance wavelengths of the filter arrays is consistent with the experimental result. This implies that the resonance wavelength of these filters can be tuned by the parameters of the HCG itself.

Asymmetric high index contrast gratings were used in a novel label-free optical biosensor design by N. Erim et al. [73] that was based on a spectrum refractive index sensing technique. Both 2D and 3D finite-difference time-domain techniques are used to characterize and assess the performance of the developed biosensor. TE polarized light waves are used to illuminate the designed sensor in-plane. The salient properties of the device are easy excitation scenario, simple measurement technique, compactness, possessing high sensitivity value (450 nm/RIU) and operating label free. The field of biochemical sensing techniques has new motivation thanks to the suggested sensor arrangement.

T. Sun et al. proposed a label-free optical biosensor that is sensitive to ligand-induced surface property variation and uses a silicon-based high-contrast grating (HCG) resonator with a spectral linewidth of roughly 500 pm [74]. The procedure creates kinetic and thermodynamic information on surface-attached antibodies and the antigens they are linked to. The sensor can detect serum cardiac troponin I, a biomarker of heart disease, to 100 pg/ml in 4 minutes and is faster and more sensitive than the current enzyme-linked immunoassays for cTnI.

Silicon nitride (Si3N4)-based one-dimensional grating structures were created by A. Shakoor et al. [75] and meet all requirements for integration with CMOS detectors. The durable, CMOS-compatible 1-D grating structures have an easily adjustable operating range in the visible to near-infrared spectrum. While the experimental linewidth is 8 nm (with 55% resonance depth), which is lowered by the detector resolution, the gratings can achieve 6 nm and 1 nm linewidths for the transverse-magnetic (TM) and transverse-electric (TE) polarizations, respectively, with 90% resonance depth. When combined with a detector, the device's experimental sensitivity of 160 nm/RIU can be transformed to an extremely high sensitivity of 1700%/RIU, making it easier to detect even the smallest changes in refractive index.

High-contrast gratings (HCGs) have emerged as an assuring technology in optical biosensing due to their design flexibility and distinctive optical properties.

Table 2.1: A summary of the advantages of HCGs in optical biosensing is given below

Author(s) & Year	Description	Advantage
A. Liu, et al., 2014 [76]	Presents high-contrast grating (HCG) structures with integrated optical sensors to improve guided mode resonance for improved sensing.	Compact design and High sensitivity, useful for various optical sensing applications.
T. Sun, 2015 [77]	Explores the design, fabrication, and application of HCG structures in optical sensing, with theoretical and experimental insights.	Provides an in-depth study of HCG principles, leading to highly sensitive optical sensors with improved performance.
Y. Takashima, 2020 [78]	Investigates GaN-based HCGs for refractive index sensing in the blue-violet wavelength range, analyzing sensitivity and effectiveness.	Enhanced sensitivity and stability in the blue-violet region, ideal for biomedical and environmental sensing.
T.T. Hoang et al. 2022 [79]	Conducted a numerical investigation of MDM (metal-dielectric-metal) plasmonic meta surface-based refractive index sensor with good contrast and sensitivity in the near-infrared range	By minimizing Ohmic losses, operating in the near-infrared area improves sensor performance. The suggested sensor offers a strong platform for biosensing applications.

G. Finco et al. 2021 [80]	Examines the effects of different HCG configurations (pedestal and half-buried) on guided-mode resonance for biosensing.	Optimized HCG designs for improved biosensor performance, enhancing sensitivity and selectivity.
L. Y. Beliaev et al., 2022 [81]	Focuses on pedestal HCG structures for biosensing, highlighting their optical properties and sensing capabilities.	Pedestal HCGs offer improved resonance characteristics, leading to better detection accuracy and higher sensitivity.

These advantages show the potential of HCGs to increase the performance of optical biosensors, offering improved quality factors, high sensitivity and versatility in design and integration.

A thorough examination of the properties of HCGs and monolithic HCGs as an optical sensor was provided by Marciniak et al. [82]. They demonstrated how the VCSEL mirror reflectivity is affected by the material's refractive index. However, the study only looked at methane absorption at a wavelength of 1651 nm; other compounds have not yet been detected. Using an HCSG structure and grating parameters (width, thickness, and grating) as well as incidence angle, Fang et al. [83] showed a polarization-independent filter that achieves high reflectivity. The reflectance of the HCSG altered when the grating period, length, and angle of light incidence all reduced.

A zinc oxide (ZnO) layer biomedical sensor, silicon nitride (Si3N4), and plasmonic gratings were combined by Elrashidi and Ali [84] to detect changes in the surrounding medium refractive index in order to detect the content of glycerol in deionized water. With a refractive index sensitivity of 806 nm/RIU, a figure of merit of 57.6, a quality factor of 57.3, and a linewidth of 14 nm, the optimal performance was obtained at a duty cycle of 35%. The sensor can be integrated into a variety of biological applications due to its high sensitivity and compatibility with CMOS devices.

Z. Gharsallah et al. [85] presented high-sensitivity and ultra-compact optical biosensor designed for detecting urea concentration. The authors utilized advanced photonic

structures to enhance the sensor's performance, ensuring precise and efficient detection. The study highlights the sensor's compact design, improved sensitivity, and potential applications in biomedical diagnostics.

Zhu *et al*. [86] investigated plasmonic RI refractive index sensors to simulate the resonance modes and sensing characteristics of these structures. The One-dimensional grating composite structure provided a sensitivity of 660 RIU/nm and a figure of merit (FOM) of 169 RIU^{-1}, while the two-dimensional grating composite structure had a higher sensitivity of 985 RIU/nm and an FOM of 298 RIU^{-1}.The 1D grating structure had the benefit of easier fabrication and 2D offered better performance. Both structures were considered useful for the creation of plasmonic refractive index sensors.

To detect refractive index (RI) on a silicon-on-insulator (SOI) substrate, M.A. Butt[87] introduced a novel asymmetric loop-terminated Mach-Zehnder interferometer (a-LT-MZI) design. Smaller configurations that operate with smaller optical equipment are made possible by a Sagnac loop, which reduces the interferometer's effective length. The subwavelength (SWG) waveguide inside the sensor arm raises the sensitivity of the proposed device from 261 nm/RIU to 510 nm/RIU.

2.3 A Survey on Surface Plasmon Resonance for Biosensing and Optical Applications

J. González-colsa et al. [88] introduced a grating-based gold metal surface that acts as a high-sensitivity sensor and a unidirectional plasmon source. Surface plasmon polaritons (SPPs), which were electromagnetic waves coupled with surface plasma oscillations and were made to be readily produced, were used in the sensor design. A maximum sensitivity of 1500 nm/RIU was attained by fixing the normal incidence for an aqueous medium in the near-infrared.

A new plasmonic refractive index (RI) sensor for biological sensing based on a complementary grating structure of silicon and gold was proposed by X. Wang et al. [89]. This sensor structure utilized surface plasmon resonance to provide a high RI sensitivity of 1642 nm/RIU for gas sensing and 1212 nm/RIU for liquid sensing. It facilitated a figure of merit of 135 $RIU^{-1}$for liquid sensing and 409 RIU^{-1} for gas sensing. The design included complementary silicon (Si) and gold (Au) gratings on a

glass substrate and had a propagation mode suitable for RI sensing. The sensor's performance was maximized by modifying the geometric parameters of the grating.

An SPR biosensor had been presented [90] comprising a PMMA photonic crystal fiber (PCF) and an indium tin oxide (ITO) for matching plasmon excitation. ITO allows operating in the telecommunication window providing tuneable properties and stability over gold or silver. The plasmonic sensor achieved a sensitivity of 2000 nm/RIU and a resolution of 5×10^{-5} RIU. Its simple design, multi-channel capability, and numerical simulation through FEM demonstrated the perspectives of using it for biosensing.

C. Lin and S. Chen [91] investigated theoretically the impact of adding a dielectric layer on the detection accuracy of SPR sensors. The authors discovered that the detection accuracy of the sensor can be improved by adding a dielectric layer whose refractive index is lower than that of the analyte. In order to shed light on the physical mechanisms underlying these advancements, they also investigate the connection between detection accuracy and the strength of the electric field at the analyte–dielectric interface.

Mishra et al. [92] introduced a theoretical investigation into a surface plasmon resonance (SPR) based fiber optic sensor that uses indium tin oxide (ITO) and silver (Ag) coatings to detect changes in the refractive index within the visible spectrum. The proposed sensor features a multi-layered design, incorporating a fiber core, an ITO layer, an Ag layer, and the surrounding sensing medium. This optimized sensor configuration demonstrates a high figure of merit (FOM) and an enhanced electric field, which leads to high immunity to electromagnetic noise, compatibility with optical fibers, stability, and low cost.

B.Raj et al.[93] presented organic field effect transistors that utilize organic compounds as semiconductors. Even though they are perfect for flexible and wearable electronics, such as biosensors. Due to their sensitivity to changes in the environment, that makes them promising for sophisticated sensing applications.

Table 2.2: Shows the comparison of the sensitivity of the various types of SPR sensors reported in the previous literature with the proposed structure's sensitivity. It also shows the simulated structure is superior to others.

Ref. No.	Sensor Utilized	Technique/Characteristics	Sensitivity (nm-RIU^{-1})
[94]	Internal-coated SPR	Conducting metal oxide film for IR region	1310
[95]	Internal-coated SPR	Tapered optical fibers for the visible region	2000
[96]	Internal-coated SPR	Double resonance dips	1929
[97]	Internal-coated SPR	Birefringent microstructure optical fiber	3100
[98]	External-coated SPR	D-shaped fiber with a solid core	2000
[99]	External-coated SPR	Multi-hole fibre	2000

2.4 Gaps in the Present Study

- High Sensitivity and Selectivity are the major challenges in the Optical Biosensors [100]. To attain both high sensitivity and selectivity needs optimizing the sensor's design material choice, structure, and surface chemistry. Highly sensitive designs may discover unwanted signals, reducing selectivity. Sensitivity and selectivity [101] balancing are critical for reliable biosensing in medical diagnostics and environmental monitoring. This necessitates a material selection, careful optimization of sensor design, surface chemistry and structural configuration.
- Point-of-care capability and low cost is another issue [102].

- Comparative research of different kinds of nanomaterials has not been analyzed in previous studies. To further enhance the sensitivity and resolution, more research is required on the plasmonic nanoparticles.[103]
- Miniaturization of optical transduction methods for portability. Minimizing optical systems to establish portable biosensors is a major issue without sacrificing performance [104].
- In some instances, there is very little peak wavelength shift concerning the refractive index change making it difficult to measure and detect accurately.
- Researchers may define which materials significantly enhance optical biosensors' sensitivity and detection accuracy by conducting comprehensive investigations. Discovering efficient materials would result in better biosensor designs with accurate and dependable biological detection [105].
- The high-Q-factor defect mode necessitates the adoption of large structures that decrease the coupling of light into and out of the sensor to achieve high reflectivity around the defect.
- Furthermore, enhancing the tunability of plasmonic effects for several sensing purposes is still challenging, specifically in materials with tuneable characteristics like ITO [106]. Important issues include long-term stability and repeatability and the requirement to properly understand the variables affecting sensor drift and degrading over time specifically under difficult conditions. Simultaneous detection of different analytes would be useful for real-world applications. These shortcomings present significant opportunities for plasmonic sensor design.

2.5 Objectives of thesis

1. To analyze the various optical parameters effect on two-dimensional high-contrast sub-wavelength grating structure.
2. To design model of high contrast grating sensor with improved sensitivity and quality factor.
3. To validate and enhance the designed structure of high contrast grating for different optical biosensing applications.

2.6 Research Methodology

The study started with a thorough review of the literature, which included books, journals with SCI indexes, and pertinent data from reliable sources. Developing an adequate understanding of the current developments and difficulties in High Contrast Grating (HCG) structures is the aim of this survey, especially about optical and biosensing applications. This study intends to build a strong basis for tackling the stated goals and making innovative contributions to the area by gathering insightful information from a variety of sources. A thorough theoretical examination of the various geometrical parameters of HCG has been carried out. These factors, which are crucial in determining the grating's optical response, are the grating period, grating thickness, filling factor, and refractive index contrast. Optimizing HCG designs for optimal reflectivity, effective waveguiding, and improved sensing capabilities requires an understanding of these characteristics. We will thoroughly examine how these structural differences affect HCG's performance in optical and biosensing applications.

The Finite-Difference Time-Domain (FDTD) method and COMSOL Multiphysics are two of the software tools and computational approaches that will be used to ensure accurate simulation and validation of HCG structures. These techniques allow for a detailed assessment of the optical properties of the planned gratings by accurately modeling the passage of electromagnetic waves through them. To make sure that HCG structures are optimized for their intended uses, the numerical simulations will offer crucial insights into their resonant behaviour, reflection spectra, and field distribution. Additionally, real-world biosensing applications must be used to validate the planned HCG specimen. This entails evaluating its accuracy, sensitivity, and specificity in identifying different biomarkers. By combining the manufactured HCG structures with a biosensing apparatus and examining how they interact with biological materials, experimental validation will be completed. In order to objectively analyze the efficacy of HCG for biosensing, characteristics such resonance wavelength shifts and constraints on detection will be evaluated.

Advanced data analysis tools will be used for post-processing and comparative examination of the developed HCG structures. Numerous factors, including sensitivity, reflectivity, detection accuracy, and fabrication feasibility, will be taken into consideration when evaluating the various configurations. The outcomes of these

analyses will help determine the most effective and adaptable HCG structure for a variety of uses, such as optical communication, environmental monitoring, and medical diagnostics.

A comprehensive structure for optimizing HCG designs will be created by integrating theoretical analysis, numerical simulations, experimental validation, and comparative evaluation. Future developments in nanophotonic sensing technologies will benefit greatly from the knowledge gathered from this work, opening the door to creative solutions in photonic engineering, biology, and healthcare.

2.6 Contribution of Thesis

Through this research, several key findings and contributions are presented. The sensitivity can be further enhanced by optimizing the various High contrast grating designs, HCG HCG-based plasmonic and material properties. Firstly, it is shown that HCGs offer significantly higher sensitivity compared to conventional biosensors due to their ability to generate resonant interactions with incident light. Secondly, the importance of bio-functionalization in ensuring the specificity and selectivity of the sensors is emphasized, with potential strategies for improving bio-recognition layers discussed. Thirdly, the integration of HCG sensors into practical biomedical devices, such as portable diagnostic tools and wearable health monitors, is explored, highlighting their potential to transform healthcare delivery.

CHAPTER 3

PERFORMANCE ANALYSIS OF HIGH CONTRAST SUB WAVELENGTH GRATING

3.1 Introduction

High-contrast gratings (HCGs) are sophisticated optical structures that are distinguished by a periodic arrangement of low-refractive-index areas, like air, and high-refractive-index materials, like silicon. Because of the significant refractive index contrast this arrangement of HCG structure can control light with remarkable effectiveness. The structural characteristics of an HCG are the grating thickness (h), duty cycle (defined as the ratio of the grating width to the period), and period (Λ), which is the spacing between adjacent grating lines. The grating's optical behaviour is largely determined by these characteristics. The grating's resonance wavelength is directly influenced by the period (Λ). Because of their exceptional optical qualities and high index contrast, HCGs stand out from conventional gratings and are therefore appealing for a variety of integrated optoelectronic device applications. To determine the reflectivity and transmission spectra by matching boundary conditions, the analysis typically considers three zones that are divided by the HCG input and output planes. It focuses on the lateral field components. Theoretical treatments often start with transverse magnetic (TM) polarized incidence and then move on to transverse electric (TE) polarization, pointing out the variations caused by Maxwell's equations for simplicity's sake. These analytical solutions have very efficient convergence; they frequently only need two modes to agree well with rigorous numerical simulations such as Rigorous Coupled Wave Analysis (RCWA).

A few modes are excited upon plane wave incidence in the grating bars, which can be thought of as a periodic array of waveguides. Higher-order modes are evanescent, and only two modes usually carry energy and have real propagation constants in the domain of interest [15]. It has been found that phase selection rules make it easier to comprehend and construct HCGs for optical functions. These guidelines provide an easy-to-understand design algorithm by connecting the grating mode phases to the overall reflectivity and transmission properties. The coupling between these modes is

indicated by crossings and anti-crossings in the parameter space (e.g., wavelength vs. thickness), which can be utilized to construct HCGs with desired characteristics.

Because of their special qualities, HCGs have found widespread use in a variety of optical domains. HCGs replace conventional distributed Bragg reflectors (DBRs) as high-reflectivity mirrors in vertical-cavity surface-emitting lasers (VCSELs) [24]. In addition to lowering the mirror structure's thickness and complexity, this swap improves the laser's performance by increasing reflectivity and bandwidth. HCGs are also utilized in the construction of optical filters and resonators, where their capacity to facilitate guided-mode resonances allows for the development of instruments with high sensitivity and narrow linewidths, which are crucial for spectroscopy and telecommunications applications [107].

The first objective of this research is to analyze the effects of various optical parameters on a two-dimensional High-Contrast Sub-Wavelength Grating (HCSG) structure has been achieved in this chapter. For a variety of ideal parameter values, such as modes, incidence angles, grating parameters (widths, periods, thickness), and refractive index, the reflectivity of the HCSG structure is examined. However, analysis for high reflectivity through parameter modification has been the subject of much research. Opti FDTD software can be used to easily design the proposed HCSG structure without the need for numerical calculations. It is easily implementable as a biosensing application with its optimal parameters.

3.2 Design methodology and analysis

Figure 3.1 displays the recommended schematic framework of a sub wavelength grating based on high contrast on a silicon dioxide substrate with ideal design parameters that effect the structure reflectance. The parameters consist of the grating parameters (grating thickness (tg), grating width (S), low index layer thickness (tl), grating period (L)) and its surrounding materials (index) and filling factor (F).

The ratio of the high index material's width S to the grating period L is known as the filling factor F. Underlying substance SiO2 has a refractive index of 1.47, whereas grating material Si has an index of 3.47. The SiO2-based HCSG structure is 8.5 μm wide and has a 0.460 μm-thick silicon rectangular grating. The low index material height is 1μm

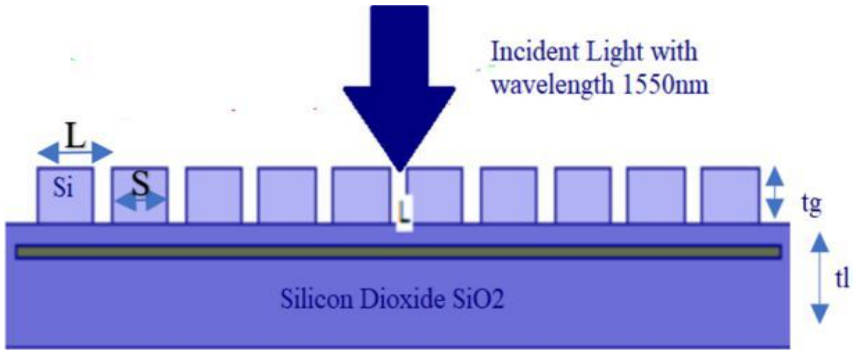

Figure 3.1: Proposed framework of sub wavelength grating using wavelength λ = 1550 nm with normal angle of incidence

When a typical light beam with a wavelength of λ = 1550 nm meets the grating, it excites several array propagation modes. After starting in the plane at z = 0, these propagating modes descend to the output plane, where z = t. They can either be sent in the same direction and escape from the output plane, or they can be reflected to the input plane. Both transmission and reflection of light are made possible by zero-order diffraction. Opti FDTD simulation tool is used for analysis of grating structure. In FDTD simulation, a continuous wave with a mesh size of 15 nm and a wavelength λ of 1550 nm excites the electromagnetic field in the grating.

In the grating, zero-order diffraction occurs when the period of grating is significantly smaller than the input wavelength. Emission and reflection of electromagnetic waves occur when λ-wavelength light strikes the grating at an incidence angle of θ. A reflectivity spectrum for the HCSG structure and zeroth order diffraction are produced when the grating is activated by TE and TM polarized modes.

3.3. Simulation Results

3.3.1. Polarization modes effects on HCSG structure

In order to analyze the performance of the suggested high contrast subwavelength grating (HCSG) framework, especially with regard to its reflectivity properties, several parameters are used. One or two specific wavelength spots have been found to have extraordinarily high reflectivity in the Transverse Magnetic (TM) mode, which is the subject of this investigation. This phenomenon is of significant interest as it determines the grating's efficiency in optical applications such as wavelength-selective reflectors, optical filters, and biosensors. Important factors such as the grating thickness, grating

period, and grating width have a major impact on the reflectance of the grating structure. Every one of these factors influences how incident light interacts with the structure, influencing whether it can transmit or reflect specific wavelengths.

The values of the grating parameters at the various polarization modes that determine the grating's reflecting properties are listed in Table 3.1.

Table 3.1: Various polarization modes' grating parameters.

Polarization	**Wavelength**	**Grating period**	**Thickness**	**Grating width**
	λ [nm]	L [µm]	t_g [µm]	S [µm]
TE	1550	0.780	0.460	0.5860
TM	1550	0.780	0.460	0.5860

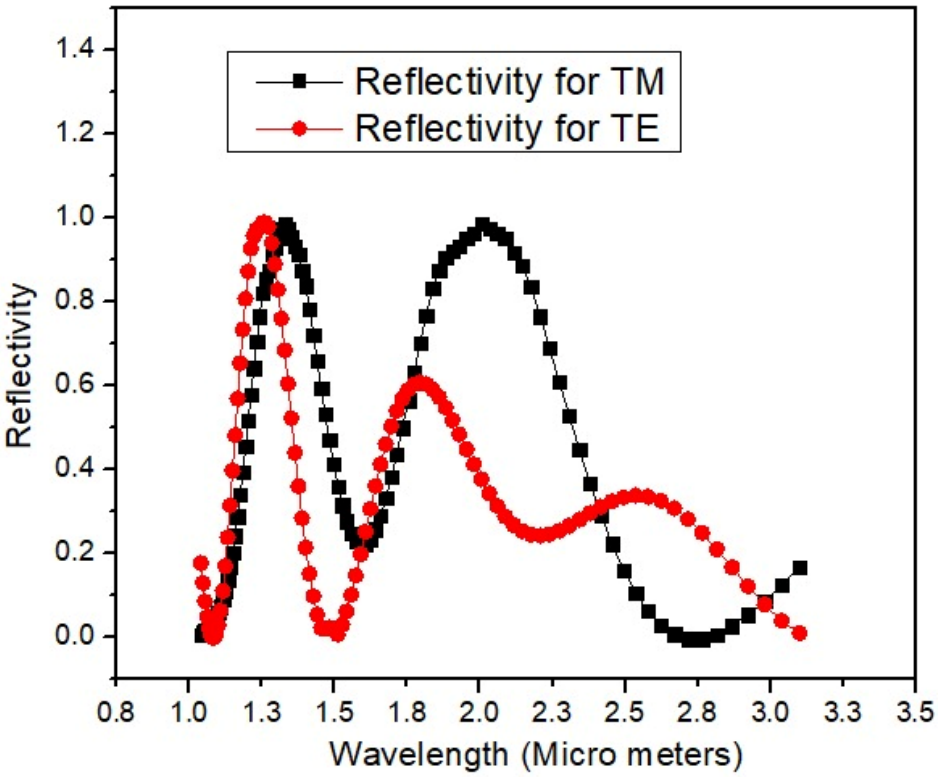

Figure 3.2: HCSG design power reflectance for TE and TM modes.

Figure 3.2 illustrates the reflectance comparison utilizing optimized grating parameters for both Transverse Magnetic (TM) and Transverse Electric (TE) modes. Both polarization modes show very high reflectivity in the 96–99.9% range, according to the research, verifying the high contrast subwavelength grating (HCSG) structure's effectiveness. More specifically, the wavelength ranges of 1.26 to 1.30 μm and 2.01 to 2.18 μm are where the TM mode exhibits the highest reflectivity. On the other hand, TE mode achieved high reflectivity in the slightly different wavelength range of 1.23 to 1.29 μm.

These variations occur because of distinct polarization conditions that affect how electromagnetic waves interact with the grating structure. The grating period, grating thickness, and fill factor structural characteristics of the HCSG—have a significant impact on these reflectivity results. The grating period must be small while maintaining the grating thickness in the HCSG design greater in order to ensure the best reflectivity performance in the TM mode. Greater reflectivity is achieved by increasing constructive interference at the grating interface, whereas a larger grating thickness improves reflectivity by strengthening the confinement of the electromagnetic field over a smaller period.

Due to the carefully optimized grating design of the High Contrast Subwavelength Grating (HCSG), the TE mode is most effective within the wavelength range of 1.23 to 1.29 μm. This means that within this specific range, the grating efficiently reflects incident light, ensuring minimal losses and improved optical performance. However, when it comes to achieving the highest possible reflectivity, the TM mode exhibits superior performance under specific structural conditions. For optimal reflection, the grating period needs to be relatively small, while the grating thickness should be sufficiently large. This combination enhances the confinement of electromagnetic waves, leading to stronger resonance effects and improved reflectivity.

3.3.2. Effect of different angles of incidences on grating's reflectivity

The High Contrast Subwavelength Grating (HCSG) structure's reflectivity performance has been examined for a range of incidence angles between 1.033 and 3.1 μm. Figure 3.3 shows the outcomes of the simulated reflectance that were acquired using the Opti-FDTD software. The impact of several incidence angles (0°, 4°, 6°, 8°, and 10°) on the grating's reflectivity is shown in the figure. As the incidence angle increases, the

positions of the two distinct resonance peaks move toward longer wavelengths has been observed. The grating's angle-dependent dispersion properties, which affect the phase-matching requirements for high reflectivity, are responsible for this change.

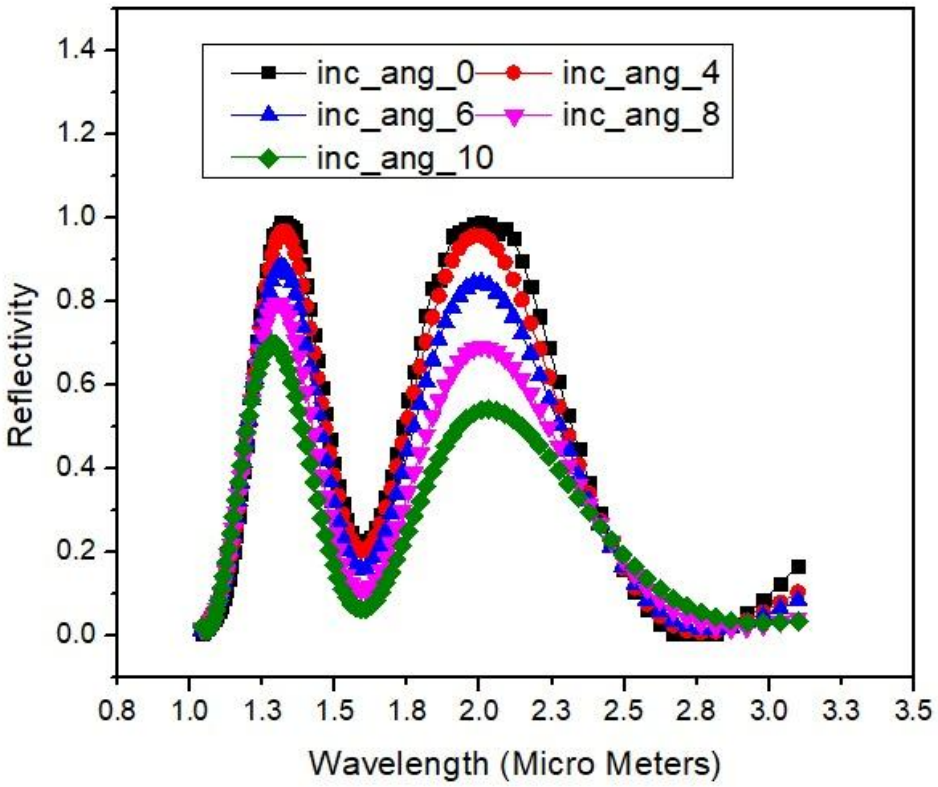

Figure 3.3: HCSG design's power reflectance at various incidence angles.

As seen in Figure 3.3, the reflectivity peaks at normal incidence (0°), attaining a reflectivity of over 99.998%. For an incidence angle of 4°, a comparable high reflectivity can be observed, suggesting that the HCSG design successfully preserves its reflecting qualities within this angular range. Reflectivity does, however, decrease when the angle rises over 4°, especially between 8° and 10°, where a notable decrease in reflection efficiency is seen. The grating is especially well-suited for applications needing high reflection stability under near-normal incidence situations

3.3.3. Grating parameters effects on reflectivity

Many grating factors that affect its reflective properties, including as width, thickness, and period, have been simulated. Figure 3.4 displays the HCSG performance for various grating widths based on power reflectance at 0 degrees of incidence. A change in reflectance is shown by the size of the grating width S increasing from

0.3855 to 0.4855 µm, then changing to 0.5855 and 0.6355 µm. It is discovered that reflectivity increases up to a certain point, 0.5855 µm, beyond which it sharply decreases. A wavelength shift toward the high-wavelength sides of around 0.12 µm is also present.

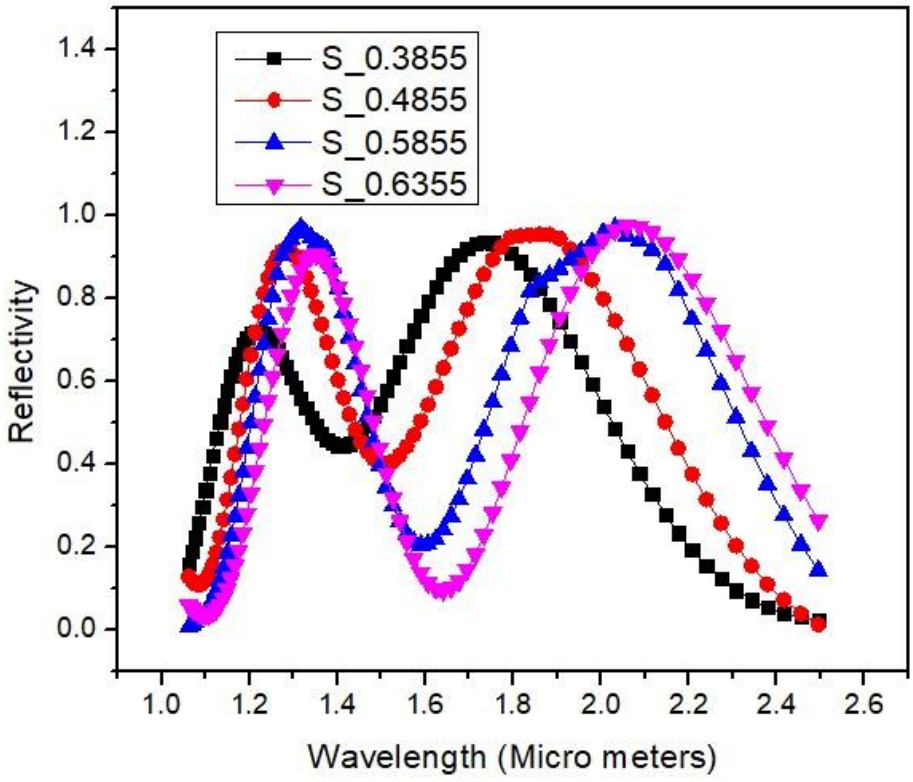

Figure 3.4: Plot for reflectivity *vs.* the wavelength for different grating widths

The effect of different grating thicknesses on the proposed sensor's reflectance performance is shown in Figure 3.5. The study examines how thickness changes between 0.455 µm and 0.502 µm affect reflectance at various wavelengths. According to the observed data, the peak reflectivity values at the two main wavelength ranges—between 1.32 µm and 1.41 µm and between 1.91 µm and 2.012 µm—remain comparatively steady despite the change in thickness. However, there is a discernible wavelength shift towards longer wavelengths as the grating thickness increases, suggesting a change in the structure's resonance conditions.

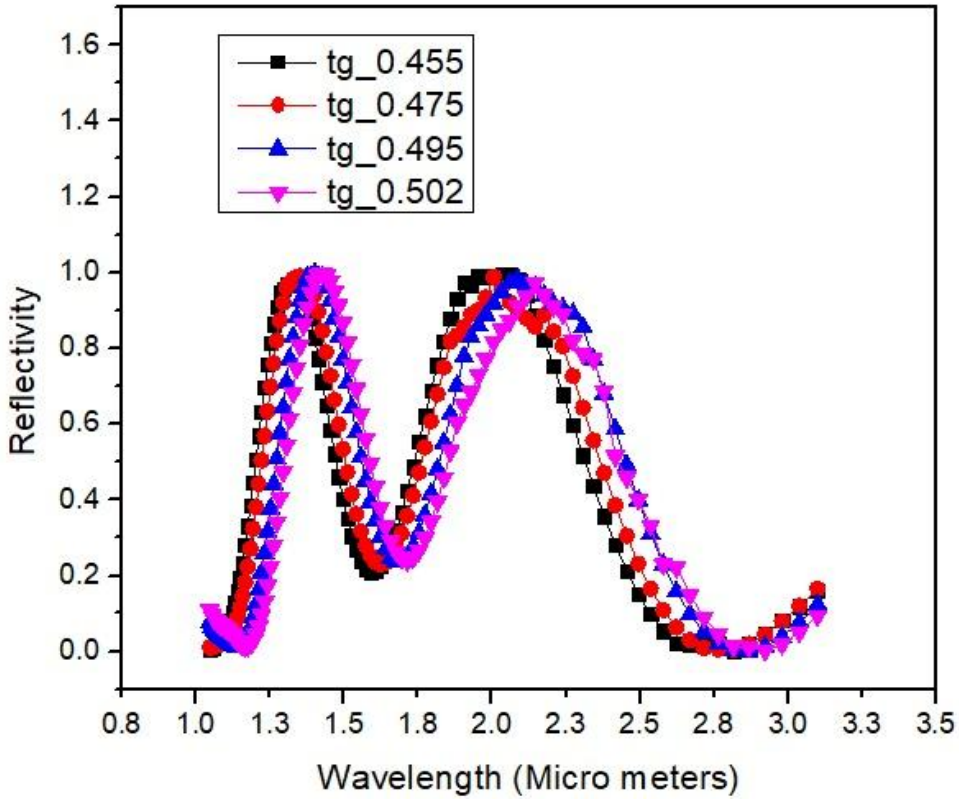

Figure 3.5: Plot for reflectivity *vs.* the wavelength for different grating thicknesses

The impact of changing the grating period on the designed structure's reflectivity performance is shown in Figure 3.6. The graph illustrates how the reflectivity spectrum changes as the grating period increases by comparing three distinct grating periods: 0.77 µm, 0.87 µm, and 0.97 µm. The plot clearly shows that the structure with the best reflectivity throughout both major resonance peaks, especially in the lower wavelength area between 1.3 µm and 1.4 µm, has a grating period of 0.77 µm. A slight decrease in reflectivity and a shift in the resonance peak positions toward longer wavelengths are seen as the grating period increases to 0.87 µm and 0.97 µm.

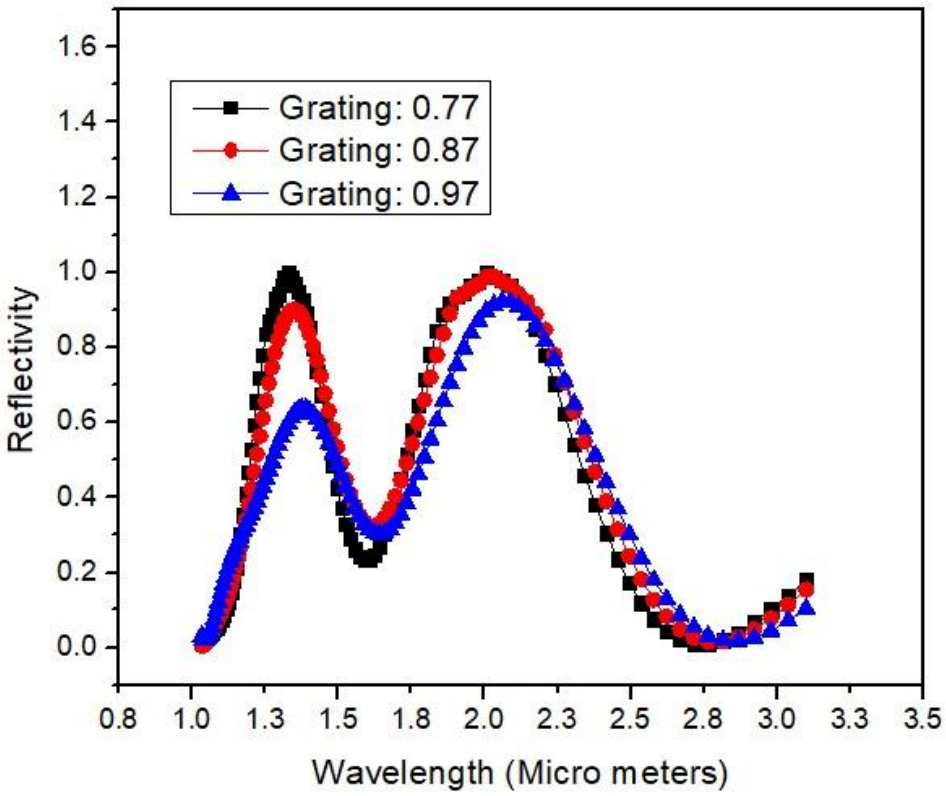

Figure 3.6: Plot for reflectivity *vs.* the wavelength for different grating periods

3.3.4. Various refractive indexes effects on grating

A variable refractive index of the surrounding media above the grating has been used to observe the reflectivity of HCSG.

The results for HCSG with different surrounding refractive indices (R.I.)—that is, R.I. = 1, R.I. = 1.2, R.I. = 1.3, and R.I. = 1.35—are shown in Figure 3.7. A shift in the surrounding refractive index causes a wavelength variation in the reflectivity drop. Applications for high-contrast subwavelength gratings in biosensing can benefit from this feature.

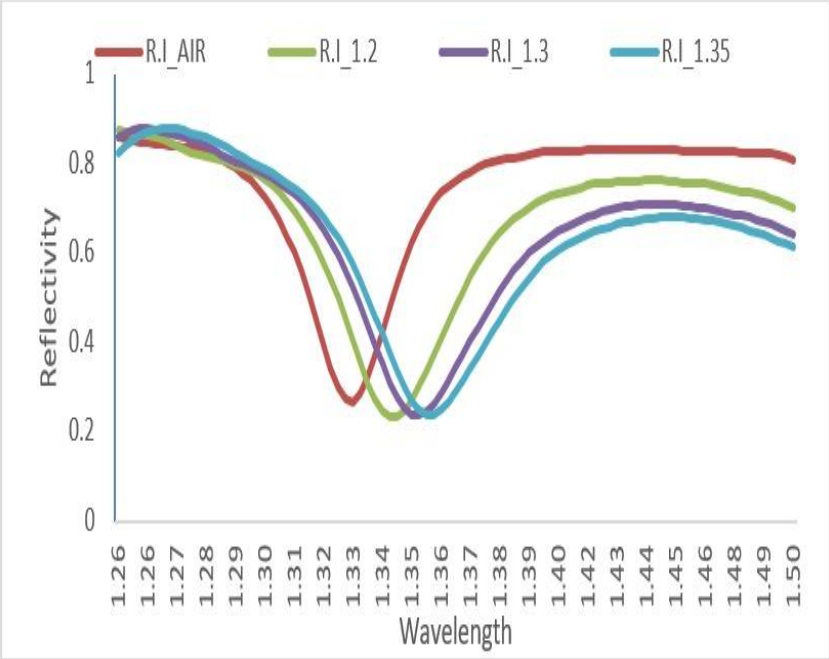

(a)

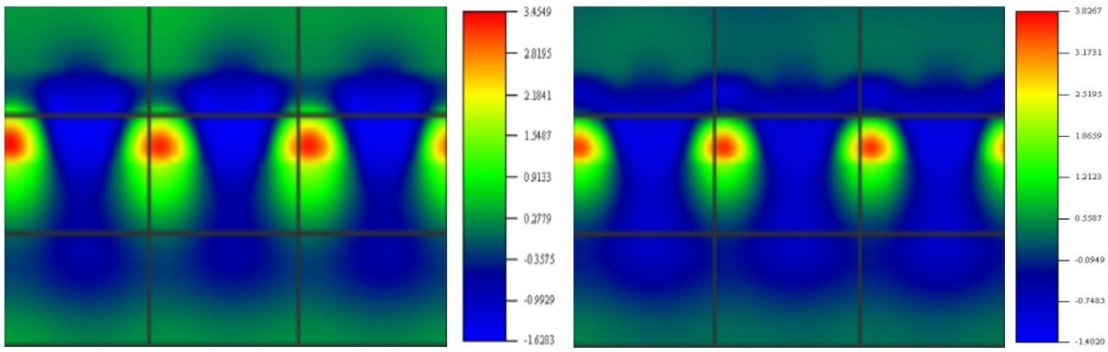

(b)

Figure 3.7(a): HCSG with different surrounding refractive indices (b) HCSG's optical field distribution at different refractive indices.

The achieved outcomes of the light intensity distribution in the HCSG sensor with R.I. = 1.0 and R.I. = 1.2 are displayed in Figure 3.7 (b) It has been noted that when the surrounding refractive index rises, the light intensity inside the grating falls.

Table 3.2: Comparison of proposed reflectivity with values reported in the literature.

Research Paper	Power Reflectance (%)
Reported in [108]	85.00
Reported in [109]	83.20
Proposed	**99.998**

While the suggested structure produces high reflectivity, documented low reflectivity values of 85% [95] and 83.2% [96] are found. Therefore, Table 3.2 compares results with previously published literature to demonstrate the structure's superiority.

The sensitivity of HCSG is the ratio of change in resonance wavelength to change in refractive index. It has been observed that the sensitivity of the HCSG grating design is 900nm/RIU. The quality factor (Q) is defined as the ratio of resonance wavelength and full wave half maxima and it has been observed at about 255 for the grating structure. Achieving high detection resolution in refractive index sensing applications requires that the resonance retain its sharpness, as seen by the comparatively constant Q-factor across a range of indices.

3.5 Conclusion

The High-Contrast Subwavelength Grating (HCSG) structure was thoroughly examined to maximize its performance parameters and get ultra-high reflectivity. After doing a thorough series of calculations and design iterations, the best arrangement for the HCSG structure would optimize its reflecting qualities. The best-optimized parameters in our research for HCSG structure are the polarization mode (TM mode), angle of incidence (0°,4°), grating width (S = 0.5855 μm), grating thickness (tg = 0.495 μm), and grating period (L = 0.77 μm). Together with these considerations, a wavelength of reflectivity dip moves to the right when the surrounding material's refractive index changes. All these properties combine to give the HCSG structure a reflectivity of 99.998%, which can be used in biosensing applications.

Additionally, it was shown that when the refractive index of the surrounding material rises, the reflectivity dip wavelength redshifts, or shifts toward longer wavelengths. Because even slight changes in the refractive index can be detected up by the corresponding shift in the resonance wavelength, this characteristic is especially useful for sensing applications. The simulated reflectivity achieves a remarkable 99.998% under ideal circumstances. A high-Q resonance, which is necessary for applications requiring accurate and extremely sensitive optical feedback mechanisms, such as biosensing, filtering, and optical communication systems, is indicated by such a high reflectivity.

CHAPTER 4

ANALYSIS OF HIGH CONTRAST GRATING BIOSENSOR USING SURFACE PLASMON RESONANCE

4.1 Introduction

The phenomena occurring in surface plasmon resonance (SPR) waveguides improve the pattern of biosensors in terms of sensitivity, robustness, and compactness. The theory behind the SPR waveguide concept includes the electromagnetic wave theory. In all photonic integrated circuits [110], the propagation of light or electromagnetic waves is a significant aspect [111]. To achieve good selectivity and sensitivity, the selection of material (i.e., dielectric or metal) having good optical properties (reflectance and transmittance) has gained attention from the research fraternity [112]. Many groups of researchers have explored the optical properties of many metamaterials. Further, the miniaturization of dimensions or structures of photonic devices has also been achieved in patterning [113]. During the past few years, the discovery of near-wavelength grating structures has proliferated. The medium of high index is constrained by low-index materials mentioned as an HCS i.e. high contrast subwavelength grating. Further, technology advancement in lithography researchers contributed actively in the field of High Contrast Grating.

In 2017, we proposed a novel grating multilayer-based biosensor prototype to detect lung cancer using the Vroman effect [114]. Zhuo Li et al. [115] demonstrated the HCG-based SPPW (spoof surface plasmon resonance waveguide) which further opened a window for ultra-low loss SPP waveguides. They also elaborated that HCG-based SPPs are much better than metal grating-based SPPs subject to the geometry and medium parameters engineering. In continuation of that, HCG also shows properties to be a prominent biosensor [116]. Fang et al. [117] demonstrated a polarization-independent filter using an HCSG structure to achieve high reflectivity using grating width, thickness, periods, and angle of incidence. As grating parameters increase and the angle of incidence decreases, the reflectivity of the HCSG structure increases. The bimetallic layered structure using high contrast grating has a good penetration depth of surface plasmon modes in the dielectric region [118]. Better computational techniques made it easier to understand the behaviour of plasmonic modes in HCG. Similarly, it has been

easier to fabricate metallic HCG for biosensing applications [119]. It is represented in the study presented in [120] that high-quality factors can be achieved by optimizing the grating period, duty cycle, and thickness of the substrate. Another study [121] shows that Silica-based photonic crystal slabs when utilized with graphene show superior sensing performance and can be promoted for refractive index-based sensing applications.

HCG-based sensing is helpful in many areas like HCG can be utilized to create the kinetic and thermodynamic data on antibodies that are surface-attached with the respective antigens [74]. Other study shows pedestal HCG [81] can show bulk and surface sensitivity more than the basic HCG structures. GaN-HCG-based sensor structures can help in application areas like IoT for analytical sensing [122] .

Previously, only metals have shown good dispersion characteristics as well as plasmonic behavior of Gold (Au), Silver (Ag) & Aluminium (Al), etc. But, West et al. [123] paved a new way for alternate plasmonic materials, which showed the same characteristics as plasmonic metals. Similarly, Teotia et al. [114] proposed a multi-layered bimetallic structure using a high dielectric region. Painam [124] also presented a prototype of the biochemical sensor to detect chemical concentration using a photonic crystal waveguide.

The above biosensors use different technologies of Surface plasmon resonance and a photonic crystal waveguide but have specific sensitivity and detection accuracy limitations. To meet the best configuration, we have investigated HCG-based plasmonic biosensors using Indium Tin Oxide (ITO) and Gold (Au).

4.2 Proposed Setup of HCSG using Surface Plasmon Resonance

The proposed HCG-based plasmonic biosensor is shown in Figure 4.1. It includes a layered structure having a metal surrounded by high-contrast dielectric material with efficiently managed gratings. The proposed structure of the waveguide is made up of a dielectric silica layer with a refractive index of 1.44 and another stacked dielectric silicon layer with a refractive index of 3.42. For better sensitivity and detection capability, air holes must be added in structuring HCG-based biosensors. This is also done to improve the all-over performance of the sensor. The air hole inclusion will help in increasing the interaction between the biomolecules and guided light. This will further improve the biomolecular binding and hence, the sensitivity of the sensor.

If there are no air holes, mode resonance effects will be weakened, and sharp dips will be observed. HCG air holes produce a high contrast refractive index between material and medium. If these air holes are removed, it will decrease the contrast and can create weak confinement. This will lower the overall reflectivity. Furthermore, the absence of airholes can weaken the Bragg reflection which will further reduce the efficient reflection ability of structure for certain wavelengths. Hence inclusion of air holes has a significant role.

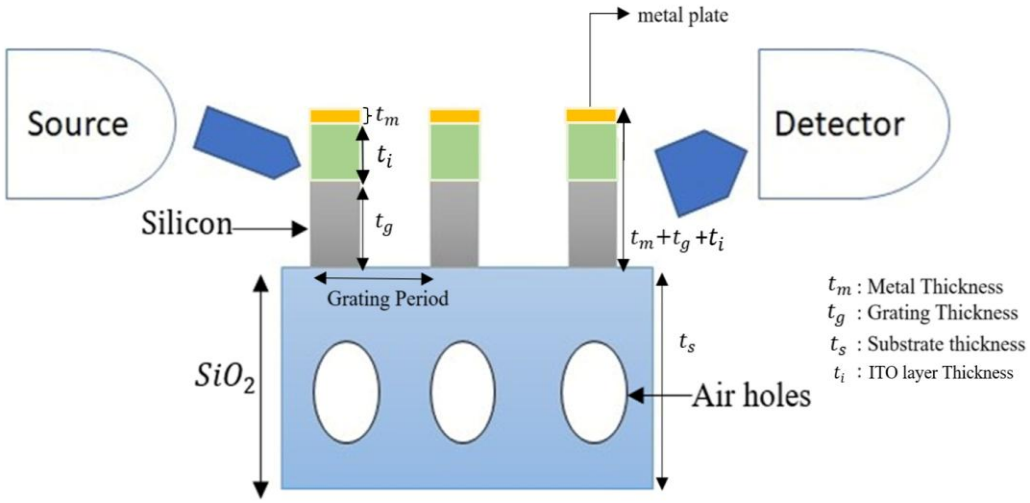

Figure 4.1: Analysis of HCG using Plasmon Resonance

The proposed structure is covered by a periodic grating of 50nm which is filled with air (η=1.0). Further, the metal layer at the top is monitored by the analyte. The proposed geometry consists of an interface of metal and dielectric, which is modulated by periodic gratings. According to the Bloch-Floquet condition shown in equation (1):

$$k_{xn} = k_x + n.\frac{2\pi}{d} \tag{4.1}$$

Floquet theorem states that a TM (Transverse Magnetic) polarised wave strikes the structure's surface as defined in Figure 4.1 with free space number i.e., k_0

($k_0 = \frac{\omega}{c_0}$, ω = wave number and c_o = velocity of light) will produce strong Bloch waves. Usually, in the SPP conditions of the sensing area, it is said that resonance wavelength is truly sensitive to refractive index variations of the analyte of the sensor (using the wavelength interrogation method) [55]. A defined ray from a light source passes through the above-said waveguide using appropriate photonic devices An

optical photodetector can detect the same light for further observations. By wavelength interrogation, a wavelength (transmission) spectrum shows a minimum value at resonance wavelength. A small change in the analyte's refractive index causes a good shift in the wavelength spectrum called refractive index sensing

Generally, the biosensor may be evaluated in terms of detection accuracy and sensitivity. Sensitivity 'Sn' can be expressed by the following equation (4.2) for 'λ': wavelength and 'RI' as refractive index [55]:

$$S_n = \frac{\delta\lambda}{\delta\,(RI)} \tag{4.2}$$

While detection accuracy can be expressed w.r.t. full width at half maximum (FWHM) by the following equation (4.3) [55]:

$$DA = \frac{1}{FWHM} \tag{4.3}$$

To approach a better design of biosensors in the case of SPP with HCG, the thickness of the metal and dielectric layer has to be determined in such a manner that the TM wave can be excited. For more understanding of p-polarised wave at the output of waveguide, an equation with respect to Flouqet theorem and Bloch waves can be expressed by equation (4.4) [125]. In equation 4.4, for studying the p-polarized light, the transmitted power P(f) is studied in terms of normalized power to source hence, it is also called normalized transmitted power as a function of frequency.

$$P(f) = e^{-4\pi\, img(n_{eff})\frac{L}{\lambda}} \tag{4.4}$$

where $\eta_{eff} = the$ effective refractive index of design. In surface plasmon resonance, the imaginary part of metal can be better responsible for a better dip in the resonance wavelength. A sequence of iterations or simulations has been done to investigate and optimize the performance of the proposed biosensor using the Finite Division Time Domain Method.

4.3 Results and Discussion

To carry out the simulations, the substrate's refractive index has been assumed as n_s = 1.0. For a better understanding of the impact of the metal layer with high contrast grating, the following variations have been observed (i) gratings with ITO and (ii)

gratings with Au-ITO, including the parameters mentioned above. The dielectric constants for Gold (Au), ITO, Silica, and Silicon (Si) are referred from Palik et al. [126].

The Magnetic field H_y has been observed about the variation of metal layers as shown in Figure 4.2 shows that as the metal layer increases, the depth of surface plasmon waves has also increased. As already mentioned earlier, the High contrast grating provides strong SPP waves at the metal and dielectric interface.

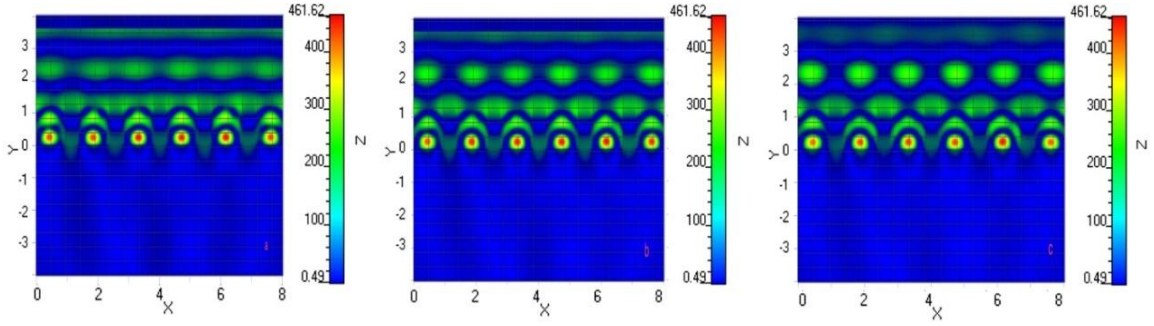

Figure 4.2: Variation of surface plasmons at a different thickness (a) 40nm (b) 50nm (c) 60nm

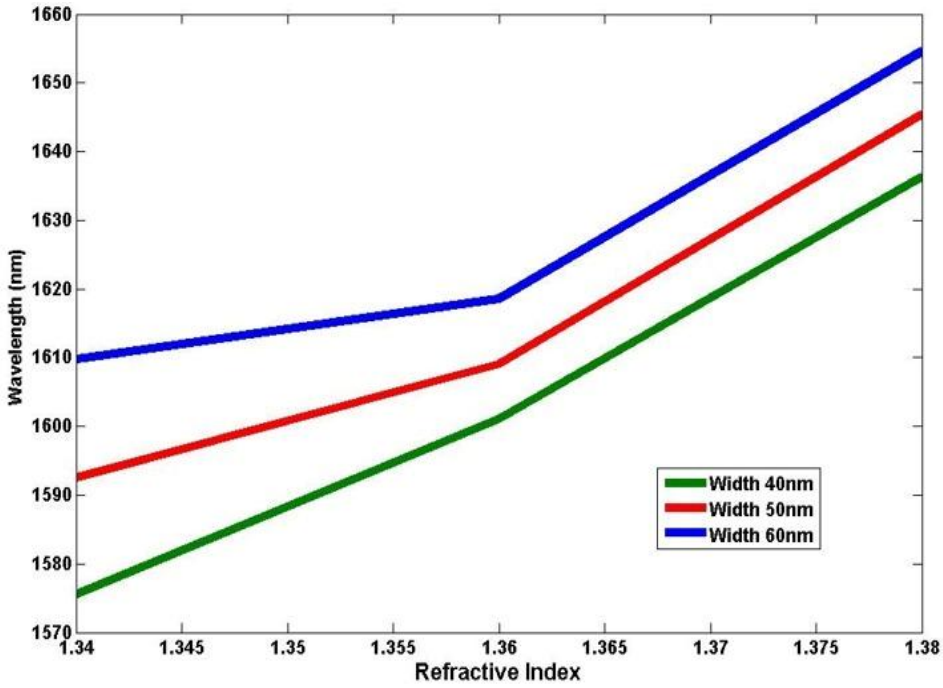

Figure 4.3: Graphical variation in resonance wavelength with metal thickness w.r.t. refractive index

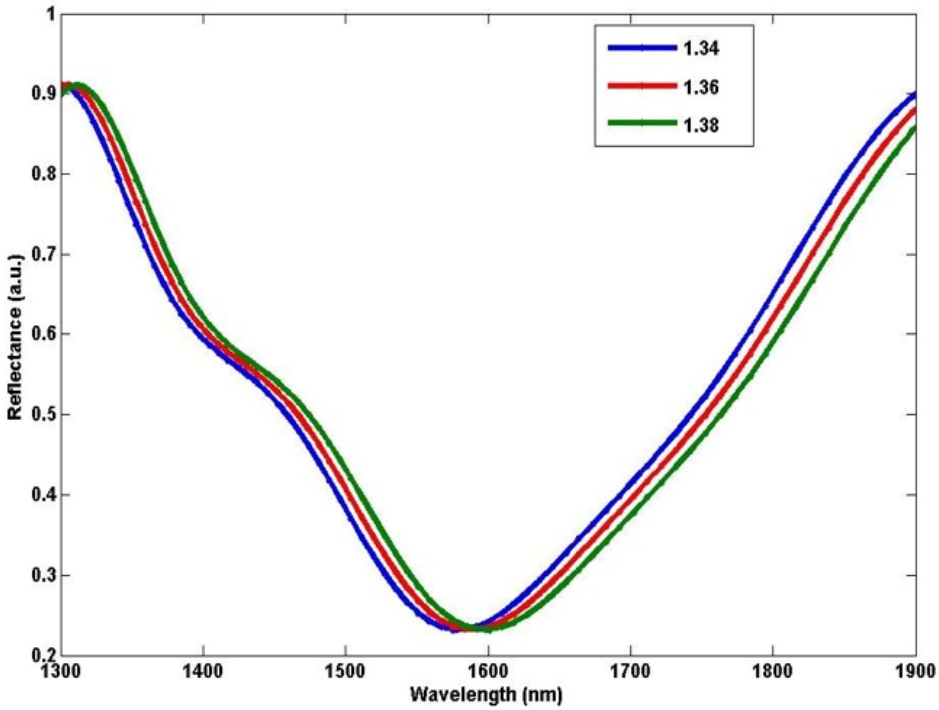

Figure 4.4: Reflectance of HCG-Based Biosensor at n=1.34,1.35 and 1.36

Further, the reflectance was also calculated by taking specific parameters constant, as shown in Figure 4.4. It has been assumed that the interaction length is almost equal to the coupling wavelength. The power has been kept virtually equal to unity.

Our previous work [113,114] has figured out that many metals have sharp transmission curves, but they also have constraints in fabrication. The use of HCG makes it easier for researchers to fabricate the design much more accessible.

Generally smaller value of $\delta\lambda$ reflects the weaker interaction of surface plasmon at metal - analyte interface. The reflection response of HCG with no metal layer can depend on various factors like grating thickness, refractive index, and wavelength of the incident light. The geometry like the thickness of HCG can help in determining the resonant wavelengths where usually high reflectivity is observed. It further affects the sharpness and strength of the reflection response.

We have also shown the changes w.r.t. refractive index where the dip is observed at 1600 nm. These sharp and narrow dips at 1600 nm show that the light is properly coupled to guided modes of the grating and further indicate that it is not reflected. These types of observations help in making HCG suitable as a refractive index-based sensor.

It is observed that the stronger interactions between the analyte and the field occur at longer wavelengths. The reason for this is the penetration of the evanescent field is extended further at longer wavelengths which also helps the structure to detect the minor changes in the refractive index. Hence, higher sensitivity will be achieved.

But Figure 4.4 shows the overall value of $\delta\lambda$, which indicates the strong interaction of surface plasmons. The presence of gratings in High-contrast grating sensors not only improves the sensor characteristics but also impacts the sensitivity and stability. The insertion of the gold layer above the ITO layer enhances the sensor's performance in terms of accuracy. It is also worth mentioning that the transmittance also got reduced due to the high value of the dielectric constant, which alters the interaction of surface plasmon resonance. Still, it will not affect the Sensitivity and detection accuracy.

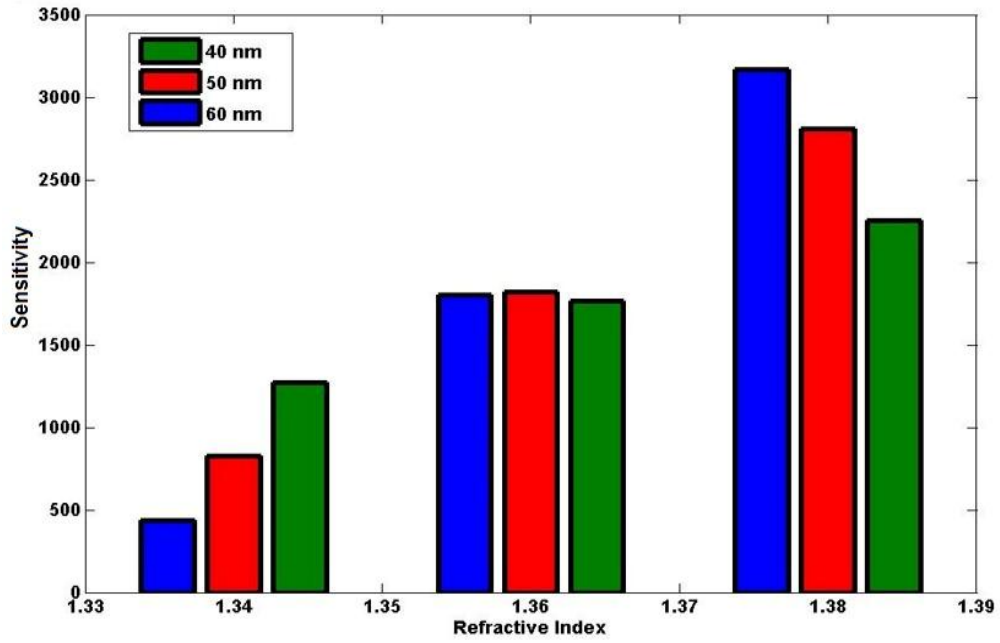

Figure 4.5: Sensitivity variation w.r.t refractive index at a different metal thickness

For more understanding of modal fields as shown in Figure. 4.2, the SPP waves have strong interaction over analyte to metal. This also shows more penetration depth than the Photonic Crystal Waveguide and Surface plasmon resonance as mentioned in [113-114]. In terms of performance, detection accuracy and sensitivity for the high contrast grating sensor have been calculated. The sensitivity is shown in Figure. 4.5, while the detection accuracy is shown in Figure 4.7. The following equation 4.5 shows the

formula for the measurement of the sensitivity of an HCG-biosensor. It is the ratio resonance wavelength shift to the unit change that occurred in the refractive index of the medium.

$$S_\lambda = \frac{\lambda_{resonance}}{\Delta\lambda} \tag{4.5}$$

Figure. 4.5 indicates that the sensitivity of the sensor increases with the thickness of the metal layer. The sensitivity at a refractive index of 1.36 was reported as 3150 nm-RIU^{-1} observations help in making HCG suitable as a refractive index-based sensor.

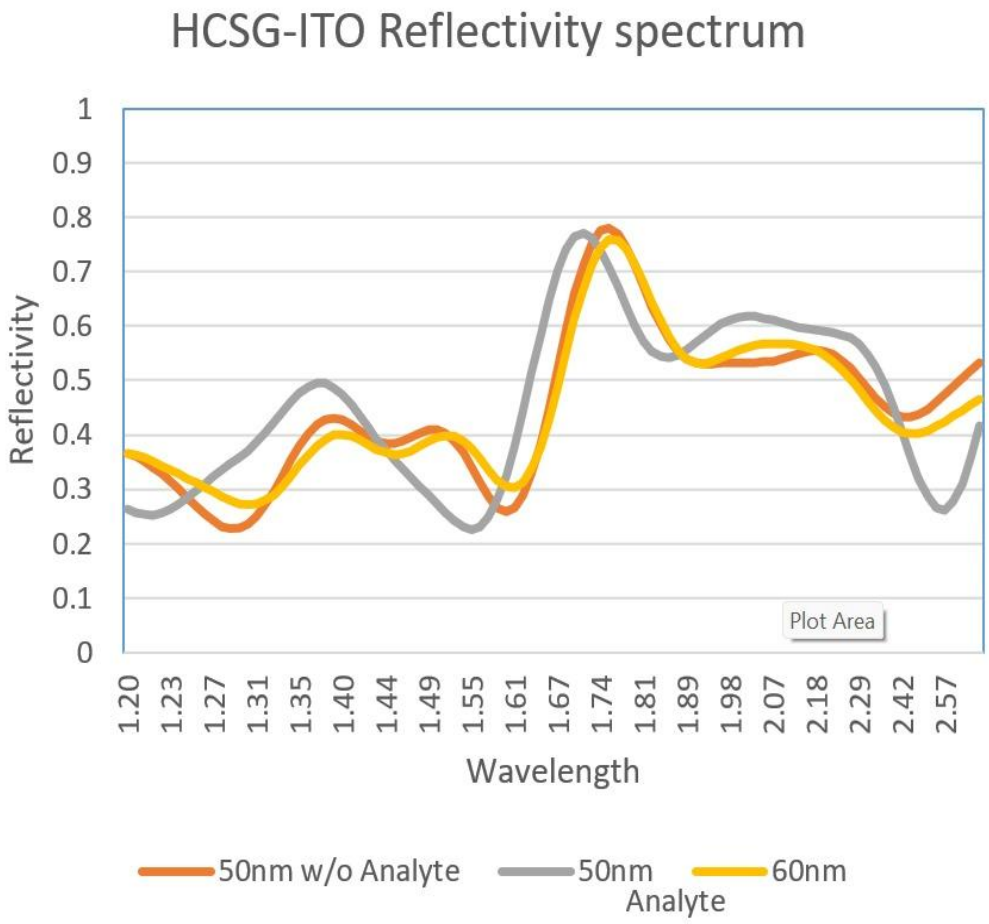

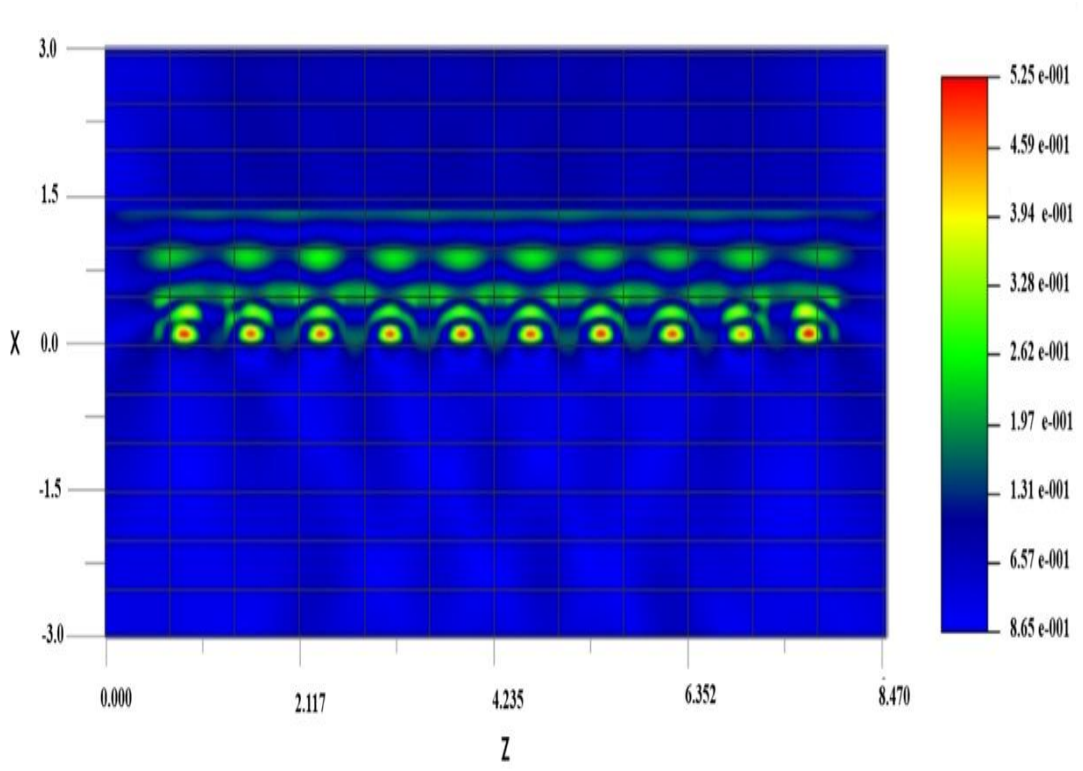

Figure 4.6: Illustration of Resonance shift with the insertion of analyte and without analyte (a) Graphical (b) EH Distribution with analyte layer

The graph in the above Figure 4.6 represents the reflectivity plot for HCSG with ITO Layer with different widths 50 nm, 60 nm, and 50 nm with analyte. From the obtained result, it has been observed that there is a wavelength shift by changing the width of the ITO layer. Another shift is observed by inserting the analyte as the top thin layer. The shift that occurred is proportional to the variation that occurred in the refractive indices which is triggered by the presence of the analyte. This happens when the analyte is bound to the surface of the sensor, it causes variation in the local refractive index. HCG-based sensors have been highly sensitive to these variations. This further causes changes in the effective refractive index of the mode, hence resulting in a resonance shift.

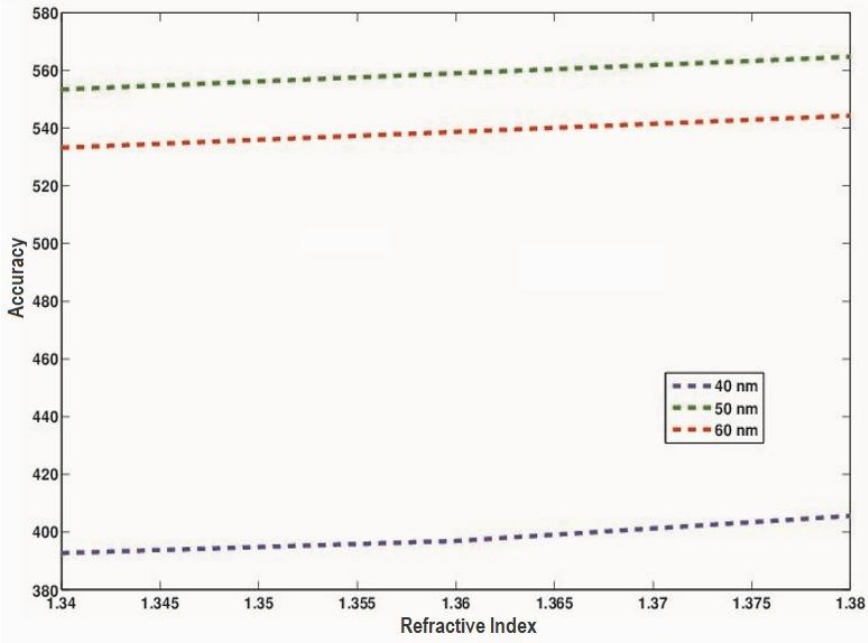

Figure 4.7: Detection accuracy variation graph w.r.t refractive index at different metal thickness

From Figure 4.7, transmittance can be described better with w.r.t sensitivity and detection accuracy at a metal thickness layer 50 nm. The detection accuracy was 560 μm^{-1} at a refractive index beyond 1.37. In comparison to the [114], a good increment in detection accuracy has been observed, while sensitivity has been slightly reduced which in turn proved a good biosensor in comparison [114].

4.4 Conclusion

High contrast grating SPP biosensors have been reported and investigated that overlap the fabrication constraints by using a high value of dielectric materials. In comparison to the Photonic crystal waveguide and surface plasmon resonance sensor, the reported sensor exhibits a higher resolution in terms of detection accuracy. High contrast grating provides stability and improves the detection accuracy 560 μm^{-1} and sensitivity 3150 nm-RIU^{-1}. The value of a high dielectric constant enhances the interaction of surface plasmon resonance and also has the lowest influence on sensitivity DA and S_n. A high value of dielectric constant and periodic grating makes it possible for this geometry to be acknowledged in any wavelength spectral domain.

CHAPTER 5

CONCLUSION RECOMMENDATIONS AND FUTURE SCOPE

5.1 Conclusion

The structural characteristics of High Contrast Subwavelength Grating (HCSG) designs have been carefully examined to maximize reflectivity. The impact of various polarization modes on HCSG reflectivity performance has been thoroughly investigated. The findings show that both TE and TM polarization modes contribute to high reflectivity; nevertheless, the degree of reflectivity for each polarization mode is mostly determined by the grating parameters, such as grating thickness, grating period, and grating breadth. These structural elements have a major effect on the efficacy and efficiency of light sources based on HCSG.

According to the results of the simulations and studies, almost 100% reflectivity is attained at an incident angle of 4° and under normal incidence (0°). The extremely careful optimization of structural parameters including grating thickness, grating breadth, and grating period is responsible for this remarkable reflectance performance. A reflectance near 100% is achieved when these values are adjusted at 0.495μm, 0.5855μm, and 0.77μm, respectively. The potential of HCSG designs in applications demanding effective optical reflectors and waveguides is demonstrated by the ability to produce such high reflectivity by simply adjusting structural parameters.

Furthermore, research has been done on how the refractive index of the surrounding medium affects HCSG reflectivity. It has been observed that the reflectivity dip shifts as the refractive index of the medium above the grating changes. One important property that can be used for biosensing applications is this wavelength shift. The presence of various biological substances in a sample can be determined by observing changes in the reflectivity spectrum. Because of this characteristic, HCSG is a good option for label-free biosensing applications, which depend on accurate biomolecular contact detection. The suggested high-contrast subwavelength grating-based biosensor shows better resolution and detection accuracy than conventional surface plasmon resonance (SPR) sensors and current photonic crystal waveguides. Improved sensor performance results from the grating material's high dielectric constant, which intensifies the interaction between incident light and surface plasmon resonance.

Additionally, the effects of detection accuracy (DA) and sensitivity (Sn) have been thoroughly investigated. The findings imply that HCSG-based sensors are very effective for practical uses since a high dielectric constant improves the interaction while having no negative impact on Sn and DA.

A multi-layered construction based on periodic HCG grating has been proposed to further enhance the biosensor's performance. Reliable biomarker detection is ensured by that design, which improves the sensor's sensitivity, detection accuracy, and selectivity. The efficiency of the biosensor is greatly increased by optimizing the grating size and metal layer thickness. Carefully adjusting the structural parameters has been found to result in a significant increase in sensitivity proportional to detection accuracy.

The suggested biosensor has a lot of potential for use in biological applications, especially in the early identification of important biomarkers like carcinoembryonic antigen (CEA). Colorectal and pancreatic cancers are among the many malignancies for which CEA is universally acknowledged as an essential biomarker. The capacity of HCSG-based biosensors to identify these biomarkers with high sensitivity and precision has the potential to transform early diagnosis and improve treatment outcomes and prognosis. Numerous structural parameter analyses of HCSG have shown its remarkable potential for use in optical and biosensing applications. It is a useful tool for many optical devices because it is possible to produce near-perfect reflectance by fine-tuning the grating parameters. Furthermore, its potential as an extremely sensitive biosensor presents encouraging prospects in the field of medical diagnostics.

5.2 Recommendations

The performance of biosensors is greatly impacted by the structural factors of HCG, such as grating period, duty cycle, and thickness. To attain the best possible figure of merit (FoM), resonance shift, and detection accuracy, future research should concentrate on numerical modeling and experimental optimization. For structure refinement, more sophisticated optimization methods like machine learning and genetic algorithms could be investigated.

Researchers should look at multi-wavelength HCG-SPR biosensors that detect several biomarkers at once by operating at different spectral bands to increase detection

efficiency. To increase sensitivity and specificity, dual-mode or hybrid sensing—for example, combining SPR with fluorescence detection could be investigated.

Real-time, low-sample-volume testing for biomedical applications can be made possible by combining HCG-SPR biosensors with microfluidic technology. This will make the technique more feasible for point-of-care diagnostics by enabling high-throughput analysis, quicker reaction times, and automation of biosensing procedures.

The surface chemistry of HCG-SPR biosensors needs to be tuned for practical biomedical applications to increase their long-term stability, specificity, and biocompatibility. To improve sensor reliability in complicated biological fluids, future research should concentrate on creating sophisticated functionalization approaches utilizing self-assembled monolayers (SAMs), nano coatings, and anti-fouling chemicals.

Enhanced sensing capabilities may result from combining HCG with other optical techniques such as photonic crystals, metamaterials, and resonant waveguide gratings (RWG). Higher sensitivity, wider spectral tunability, and an enhanced signal-to-noise ratio could all be made possible by hybrid plasmonic-photonic structures.

HCG-SPR biosensors must undergo clinical validation to close the gap between lab research and practical medicinal applications. Future research should concentrate on doing clinical trials, adhering to regulatory requirements (such as those set forth by the FDA and ISO), and guaranteeing repeatability in the identification of disease biomarkers, including those related to infectious diseases, cancer, and biomolecular interactions.

5.3 Future Scope

High contrast grating (HCG) biosensors hold great promise for advancing biological sensing when paired with surface plasmon resonance (SPR). As research in nanophotonics and biosensing advances, HCG-based sensors can improve in several crucial areas, including sensitivity, efficiency, and practicality. These sensors' high precision, real-time monitoring, and compact sensing platforms have the potential to completely transform the way diseases are detected.

One important area for further research is the examination of novel compounds for HCG structures. High-refractive-index substances (e.g., SiN_4, TiO_2) and graphene can

significantly improve light confinement, stability, and sensitivity. Excellent optical and electrical characteristics of these materials may result in enhanced biosensing application performance. Furthermore, the resilience, biocompatibility, and real-time biosensing properties of these sensors can be further improved by hybrid nanomaterials, such as metal-dielectric composites. By incorporating biocompatible materials into HCG designs, their dependability for medical applications can be greatly increased, allowing for safer and more efficient diagnostic procedures.

Another attractive line of exploration is the development of multiplexed and multi-mode HCG-SPR biosensors. The ability of conventional biosensors to identify many biomarkers simultaneously is limited since they typically only detect one wavelength. Future studies should concentrate on creating multi-wavelength HCG-SPR biosensors that can detect numerous analytes at once to diagnosis complex disorders, such as infectious diseases and cancer. Comprehensive disease profiling would be made possible by this, resulting in more precise and individualized medical care. Dual-mode biosensors that combine SPR with other optical detection methods, such fluorescence or Raman spectroscopy, can also increase specificity and accuracy, making it possible to study a wider variety of biomolecular interactions.

HCG-SPR biosensors need to be included into portable lab-on-a-chip systems and reduced in size to improve their usefulness for real-world applications. Because these sensors use microfluidic technology, which enables real-time analysis and lower sample volumes, they are ideal for point-of-care (PoC) diagnostics. These devices are useful tools for healthcare workers in distant or resource-constrained areas because of their miniaturization, which not only makes them easier to operate but also allows for quick and accurate identification. These sensors' diagnostic efficiency and accuracy can also be increased by combining them with cutting-edge data analytics and AI-driven processing. Large volumes of biosensing data can be processed by AI-based pattern recognition algorithms, allowing for more confident early illness detection.

In addition to the medical field, HCG-SPR biosensors show possibilities in food safety, pharmaceutical research, and environmental monitoring. In order to protect the public's health and safety, they can be used to identify pollutants, diseases, and toxins in food and water supplies. Additionally, by precisely monitoring molecular interactions, these

biosensors can aid in drug discovery in pharmaceutical research, hastening the creation of novel therapeutic medicines.

Future developments in nanofabrication methods will be essential to enhancing HCG-SPR biosensor performance. Sensitivity and detection limits will be further improved by the production of extremely accurate and repeatable grating structures using techniques like electron beam lithography and nanoimprint lithography. Furthermore, the incorporation of elastic and flexible substrates may facilitate the creation of wearable biosensors, which would allow patients to have their health continuously monitored.

In summary, the substantial study and advancement of HCG-SPR biosensors shows their remarkable promise for use in environmental and medicinal settings. These sensors can greatly aid in early illness detection and tailored medication by enhancing multiplexed detection capabilities, optimizing materials, and incorporating cutting-edge data analysis algorithms. The future of HCG-SPR biosensors is bright as nanotechnology develops further, opening the door for next-generation sensing platforms that have the potential to completely transform the biosensing and healthcare sectors.

REFERENCES

[1] P.N. Prasad, “Introduction to Bio photonics,” *John Wiley & Sons*, 2004.

[2] M. Shahriar, B. Rezaei, S. Ciannella, P. Yari, J. Gómez-Pastora, R. He, and K. Wu, "Advancements and perspectives in optical biosensors," *ACS Omega*, vol. 9, no. 23, pp. 24181–24202, 2024.

[3] P. Damborsky, J. Svitel, and J. Katrlik, “Optical biosensors,” *Essays in biochemistry*, vol.60, no.1, pp. 91-100, 2016.

[4] P. Han, L. Li, H. Zhang, L. Guan, C. Marques, S. Savović, B. Ortega, R. Min, and X. Li, "Low-cost plastic optical fiber sensor embedded in mattress for sleep performance monitoring," *Optical Fiber Technology*, vol. 64, p. 102541, 2021.

[5] J. Cao, T. Sun, and K. T. V. Grattan, "Gold nanorod-based localized surface plasmon resonance biosensors: A review," *Sens. Actuators B Chem.*, vol. 195, pp. 332–351, 2014.

[6] K. M. Mayer and J. H. Hafner, "Localized surface plasmon resonance sensors," *Chem. Rev.*, vol. 111, pp. 3828–3857, 2011.

[7] P. Kozma, F. Kehl, E. Ehrentreich-Forster, C. Stamm, and F. F. Bier, "Integrated planar optical waveguide interferometer biosensors: A comparative review," *Biosens. Bioelectron.*, vol. 58, pp. 287–307, 2014.

[8] N. Zaytseva, W. Miller, V. Goral, J. Hepburn, and Y. Fang, "Microfluidic resonant waveguide grating biosensor system for whole cell sensing," *Appl. Phys. Lett.*, vol. 98, p. 163703, 2011.

[9] C.R. Taitt, G.P. Anderson and F.S. Ligler, “Evanescent wave fluorescence biosensors: advances of the last decade,” *Biosensors and Bioelectronics* 76, pp.103–111,2015.

[10] R. S. Kaler, T. S. Kamal, A. K. Sharma, S. K. Arya, and R. A. Agarwala, "Large signal analysis of FM-AM conversion in dispersive optical fibers for PCM systems including second-order dispersion," *Fiber & Integrated Optics*, vol. 21, no. 3, pp. 193-203, 2002.

[11] S. K. Srivastava, A. Shalanbney, I. Khalaila, C. Gruner, B. Rauschenbach, and I. Abdulhalim, "SERS biosensor using metallic nano-sculptured thin films for the detection of endocrine disrupting compound biomarker vitellogenin," *Small*, vol. 10, pp. 3579–3587, 2014.

[12] B. C. Kress and P. Meyrueis, “Applied Digital Optics: from Micro-optics to Nano. photonics,” *Wiley*, 2009.

[13] C. F. R. Mateus, M. C. Y. Huang, Y. Deng, A. R. Neureuther, and C. J. Chang-Hasnain, “Ultrabroadband mirror using low-index cladded subwavelength grating,” *IEEE Photonics Technology Letters,* vol.16, no. 2, pp. 518-520, 2004.

[14] C.J. Chang-Hasnain, C.F.R. Mateus, and M.C.Y. Huang, “Ultra broadband mirror using subwavelength grating,” *U.S. Patent 7,304,781,* Dec., 2007.

[15] C.J. Chang-Hasnain and W. Yang, “High-contrast gratings for integrated optoelectronics,” *Advances in Optics and Photonics,* vol.4, no. 3, pp. 379-440, 2012.

[16] S. Singh, R. Kaur, and R. S. Kaler, "Photonic processing for all-optical logic gates based on semiconductor optical amplifier," *Optical Engineering*, vol. 53, no. 11, pp. 116102-1–116102-6, 2014.

[17] S.Chung, J. Mork, P. Gilet, and A. Chelno.kov, “Broadband subwavelength grating mirror and its application to vertical-cavity surface-emitting laser,” *in 10th Anniversary of International IEEE Conference on Transparent Optical Networks, ICTON,* vol. 2, pp. 101-104, 2008.

[18] H. Kaur and R. S. Kaler, "Deep learning-based port-classification approach incorporating LSTM network for high-throughput data center interconnect," *Multimedia Tools and Applications*, pp. 1-16, 2024.

[19] M.C.Y. Huang, Y. Zhou, and C.J. Chang-Hasnain, “A surface-emitting laser incorporating a high index-contrast subwavelength grating,” *Nature Photonics,* vol.1,no.2, pp. 119–122, 2007.

[20] Y. Zhou, M.C.Y. Huang, and C.J. Chang-Hasnain, “Large fabrication tolerance for VCSELs using high contrast grating,” *IEEE Photon. Technology Letter,* vol. 20, no.6, pp. 434–436, 2008.

[21] S. Boutami, B. Ben Bakir, J.L. Leclercq, and P. Viktorovitch, “Compact and polarization controlled 1:55 _m vertical-cavity surface emitting laser using single-layer photonic crystal mirror,” Appl. Phys. Lett. 91(7),071105 (2007)

[22] C.J. Chang-Hasnain, “Tunable VCSEL,” *IEEE Journal Selected Topics in Quantum Electronics,* vol. 6, no.6, pp. 978–987, 2000.

[23] M.C.Y. Huang, Y. Zhou, and C.J. Chang Hasnain, “A nano electromechanical tunable laser,” *Nature Photonics,* vol.2, no.3, pp. 180-184, 2008.

[24] H. Kaur and R. S. Kaler, "Response investigation of 3-stage 8×8 low-latency wideband TW-SOA switch for high-performance computing applications," *Optical and Quantum Electronics*, vol. 54, no. 12, p. 790, 2022.

[25] C.J. Chang-Hasnain, "High-contrast gratings as a new platform for integrated optoelectronics," *Semiconductor Science and Technology p.*014043 (2010).

[26] Z. Rahman, S. M. Zafaruddin, and V. K. Chaubey, "Performance analysis of optical wireless communications with aperture averaging over exponentiated Weibull turbulence with pointing errors," *Results in Optics*, vol. 5, p. 100171, 2021. doi: 10.1016/j.rio.2021.100171.

[27] V. Karagodsky, B. Pesala, C. Chase, W. Hofmann, F. Koyama and C.J. Chang-Hasnain, "Monolithically integrated multi-wavelength VCSEL arrays using high-contrast gratings," *Opt. Express,* vol.18,no.2, pp. 694–699, 2010.

[28] Y. Zhou, M. Moewe, J. Kern, M.C.Y. Huang and C.J. Chang-Hasnain, "Surface-normal emission of a high-Q resonator using a subwavelength high-contrast grating," *Opt. Express,* vol.16,no.22, pp. 17282–17287, 2008.

[29] V. Karagodsky, T. Tran, M. Wu, and C.J. Chang-Hasnain, "Double resonant enhancement of surface enhanced Raman scattering using high contrast grating resonators," in OSA CLEO , 2011.

[30] F. Lu, F.G. Sedgwick, V. Karagodsky, C. Chase, and C.J. Chang-Hasnain, "Planar high-numerical-aperture low-loss focusing reflectors and lenses using subwavelength high contrast gratings," *Opt. Express,* vol.18,no.12, pp. 12606–12614, 2010.

[31] Y. Zhou, V. Karagodsky, B. Pesala, F.G. Sedgwick, and C.J. Chang- Hasnain, "A novel ultra-low loss hollow-core waveguide using subwavelength high-contrast gratings," *Opt. Express,* vol.17,no.3, pp. 1508–1517, 2009.

[32] T. Sun, W. Yang, V. Karagodsky, W. Zhou, and C. Chang-Hasnain, "Low-loss slow light inside high contrast grating waveguide," in *Proc. SPIE 8270, 82700A,* 2012.

[33] T. Sun, J. Kim, J. M. Yuk, A. Zettl, F. Wang, and C. Chang-Hasnain, "Surface-normal electro-optic spatial light modulator using graphene integrated on a high-contrast grating resonator," Opt. Express, vol. 24, no. 23, p. 26035, Nov. 2016.

[34] M. Verma, R. S. Kaler, and M. Singh, "Sensitivity enhancement of Passive Infrared (PIR) sensor for motion detection," *Optik,* vol. 244, p. 167503, 2021.

[35] H. Kaur and R. S. Kaler, "XPoM-based 8-port photonic interconnection with low polarization sensitivity utilizing S–E–S hybridization," *Journal of Nonlinear Optical Physics & Materials*, vol. 32, no. 03, p. 2350030, 2023.

[36] Y. C. Liu, C. Thantrakul, S. Kan, C. Chang-Hasnain, and D. R. Ho, "Feasibility of using high-contrast grating as a point-of-care sensor for therapeutic drug monitoring of immunosuppressants," *IEEE J. Transl. Eng. Health Med.*, vol. 8, p. 2800206, Jan. 30, 2020, doi: 10.1109/JTEHM.2020.2966478.

[37] M. Tanaka, Y. Li, H. Nakajima, N. Soh, K. Nakano, K. Sakamoto, and T. Imato, "Sequential injection flow immunoassay based on surface plasmon resonance sensors: Mini-review," *J. Flow Inject. Anal.*, vol. 25, no. 2, p. 172, 2008.

[38] J. Divya, S. Selvendran, A. S. Raja, and A. Sivasubramanian, "Surface plasmon based plasmonic sensors: A review on their past, present and future," *Biosens. Bioelectron. X*, vol. 11, p. 100175, 2022.

[39] M. A. Butt, S. N. Khonina, and N. L. Kazanskiy, "Plasmonics: A necessity in the field of sensing—A review (invited)," *Fiber Integr. Opt.*, vol. 40, pp. 14–47, 2021. [CrossRef]

[40] J.J. Greffet, "Introduction to surface plasmon theory," in *Plasmonics: From Basics to Advanced Topics*, Berlin, Heidelberg: Springer, 2012, pp. 105–148

[41] R. A. Alvarez-Puebla, J.-F. Li, and X. Y. Ling, "Introduction to advances in plasmonics and its applications," *Nanoscale*, vol. 13, pp. 5935–5936, 2021. [CrossRef]

[42] L. Wu, J. Guo, H. Xu, X. Dai, and Y. Xiang, "Ultrasensitive biosensors based on long-range surface plasmon polariton and dielectric waveguide modes," *Photon. Res.*, vol. 4, pp. 262–266, 2016. [CrossRef]

[43] M. A. Butt, "Plasmonic sensors based on a metal–insulator–metal waveguide—What do we know so far?," *Sensors*, vol. 24, p. 7158, 2024. [CrossRef]

[44] M. S. Bin-Alam *et al.*, "Ultra-high-Q resonances in plasmonic metasurfaces," *Nat. Commun.*, vol. 12, p. 974, 2021. [CrossRef] [PubMed]

[45] M. A. Ismail, N. Tamchek, M. R. A. Hassan, K. D. Dambul, J. Selvaraj, N. A. Rahim, R. Sandoghchi, and F. R. M. Adikan, "A fiber Bragg grating—bimetal temperature sensor for solar panel inverters," *Sensors*, vol. 11, no. 9, pp. 8665–8673, 2011.

[46] A. V. Krasavin, P. Ginzburg, and A. V. Zayats, "Free-electron optical nonlinearities in plasmonic nanostructures: A review of the hydrodynamic description," *Laser & Photonics Reviews*, vol. 12, no. 1, p. 1700082, 2018.

[47] A. K. Sharma and B. D. Gupta, "Fiber optic sensors: A review," *Journal of Microwaves, Optoelectronics and Electromagnetic Applications*, vol. 6, no. 1, pp. 168-173, 2007.

[48] R. K. Verma, A. K. Sharma, and B. D. Gupta, "Modeling of tapered fiber optic sensor," *Optics Communications*, vol. 281, no. 6, pp. 1486-1491, 2008.

[49] A. N. Grigorenko, N. W. Roberts, M. R. Dickinson, and Y. Zhang, "Phase jumps and interferometric surface plasmon resonance imaging," *Applied Physics Letters*, vol. 75, no. 22, pp. 3295-3297, 1999.

[50] J. Homola, "Electromagnetic theory of surface plasmons," in *Surface Plasmon Resonance Based Sensors*, J. Homola, Ed. Berlin, Germany: Springer, 2006, pp. 3-44

[51] M. G. Moharam and T. K. Gaylord**,** "Diffraction analysis of dielectric surface-relief gratings," *Journal of the Optical Society of America*, vol. 72, no. 10, pp. 1385-1392, 1982.

[52] M. Masale**,** "The theory of attenuated total reflection by surface polaritons on one-sided corrugated thin films," *Optics Communications*, vol. 226, no. 1-6, pp. 1-6, 2003.

[53] U. Schröter and D. Heitmann**,** "Grating couplers for surface plasmons excited on thin metal films in the Kretschmann-Raether configuration," *Physical Review B*, vol. 60, no. 7, pp. 4992-4999, 1999.

[54] J. Homola, "Surface plasmon resonance sensors: Review," *Sensors and Actuators B: Chemical*, vol. 54, no. 1-2, pp. 3-15, 1999.

[55] Anuj K. Sharma and B. D. Gupta, "On the Sensitivity and Signal-to-Noise Ratio of a Step-Index Fiber Optic Surface Plasmon Resonance Sensor with Bimetallic Layers," *Optics Communications*, vol. 245, no. 1-6, pp. 159-169, Jan. 2005.

[56] Q.Q. Meng, X. Zhao, C.Y. Lin, S.J. Chen, Y.C. Ding, and Z.Y. Chen, "Figure of merit enhancement of a surface plasmon resonance sensor using a low-refractive-index porous silica film," *Sensors*, vol. 17, no. 8, pp. 1–9, Aug. 2017

[57] A. K. Pandey and A. K. Sharma, "Blue phosphorene/MoS_2 heterostructure based SPR sensor with enhanced sensitivity," *IEEE Photonics Technology Letters*, vol. 30, no. 1, pp. 89-92, Jan. 2018.

[58] R. S. Kaler, T. S. Kamal, A. K. Sharma, S. K. Arya, and R. A. Agarwala, "Large signal analysis of FM-AM conversion in dispersive optical fibers for PCM systems including second order dispersion," *Fiber & Integrated Optics*, vol. 21, no. 3, pp. 193–203, 2002.

[59] C.F.R. Mateus, M.C.Y. Huang, L. Chen, C.J. Chang-Hasnain, and Y. Suzuki, "Broad-band mirror (1.12–1.62 _m) using a subwavelength grating," *IEEE Photonic Technology Letters,* vol.16,no.7, pp. 1676–1678, 2004.

[60] I.S. Chung, J. Mørk, P. Gilet, and A. Chelnokov, "Subwavelength grating-mirror VCSEL with a thin oxide gap," *IEEE Photonic Technology Letters,* vol. 20, no. 2, pp. 105–107, 2008.

[61] C.J. Chang-Hasnain, Y. Zhou, M.C.Y. Huang, and C. Chase, "High-contrast grating VCSELs," *IEEE Journal of Selected Topics in Quantum Electronics,* vol.15, no.3, pp. 869–878, 2009.

[62] C. Chase, Y. Rao, W. Hofmann, and C.J. Chang-Hasnain, "1550 nm high contrast grating VCSEL," *Opt. Express,* vol.18,no.15, pp. 15461–15466, 2010.

[63] Y. Zhou, M.C.Y. Huang, C. Chase, V. Karagodsky, M. Moewe, B. Pesala, F.G. Sedgwick, and C.J. Chang-Hasnain, "High-index-contrast grating (HCG) and its applications in optoelectronic devices," *IEEE Journal of selected topics in quantum electronics,* vol.15,no.5, pp. 1485-1499, 2009.

[64] W. Yang, J. Ferrara, K. Grutter, A. Yeh, C. Chase, Y. Yue, A.E. Willner, M.C. Wu, and C.J. Chang-Hasnain, "Low loss hollow-core waveguide on a silicon substrate," *Nano.photonics,* vol.1,no.1, pp. 23–29, 2012.

[65] A. Taghizadeh, G.C. Park, J. Mørk, and I.S. Chung, "Hybrid grating reflector with high reflectivity and broad bandwidth," *Optics express,* vol.22, no.18, pp. 21175-21184, 2014.

[66] A. Liu, W. Hofmann, and D.H. Bimberg, "Two dimensional analysis of finite size high-contrast gratings for applications in VCSELs," *Optics express,* vol.22 , no.10, pp. 11804-11811, 2014.

[67] Y. Wang, D. Stellinga, A.B. Klemm, C.P. Reardon, and T.F. Krauss, "Tunable Optical Filters Based on Silicon Nitride High Contrast Gratings," *IEEE Journal of Selected Topics in Quantum Electronics*, vol.21,no.4, pp. 108-113, 2015.

[68] P. Qiao, Li Zhu, W.C. Chew, and C.J. Chang-Hasnain, “Theory and design of two-dimensional high-contrast-grating phased arrays,” *Optics Express*, vol.23, no.19, pp. 24508-24524, 2015.

[69] T. Sun, S. Kan, G. Marriot, and C. Chang-Hasnain, "High-contrast grating resonator for label-free biosensors," in *CLEO: 2015, OSA Technical Digest (online)*, Optica Publishing Group, 2015, paper STu4K.6.

[70] I.S. Chung, “Study on differences between high contrast grating reflectors for TM and TE polarizations and their impact on VCSEL designs,” *Optics Express*, vol.23, no.13, pp. 16730-16739, 2015.

[71] T. Sun, W. Yang, and C.J. Chang-Hasnain, “Surface-normal coupled four-wave mixing in a high contrast gratings resonator,” *Optics Express*, vol.23, no.23, pp. 29565-29572, 2015.

[72] A. Liu, P. Wolf, J.H. Schulze, and D. Bimberg, “Fabrication and characterization of integrable GaAs-based high-contrast grating reflector and Fabry–Perot filter array with GaInP sacrificial layer,” *IEEE Photonics Journal*, vol.8, no.1, pp. 1-9, 2016.

[73] N. Erim, M.N. Erim, D. Yılmaz, and H. Kurt, “Biosensing With Asymmetric High Refractive Index Contrast Gratings,” *IEEE Sensors Journal*, vol.16, no.20, pp. 7494-7499, 2016.

[74] T. Sun, S. Kan, G. Marriott, and C.J. Chang-Hasnain, “High-contrast grating resonators for label-free detection of disease biomarkers,” *Nature Scientific Reports*, vol.6, 2016.

[75] A. Shakoor, M. Grande, J. Grant, and D.R.S. Cumming, “One-Dimensional Silicon Nitride Grating Refractive Index Sensor Suitable for Integration with CMOS Detectors*,” IEEE Photonics Journal*, vol.9, no.1, pp. 1-11, 2017.

[76] A. Liu, W. H. E. Hofmann, and D. H. Bimberg, "Integrated high-contrast-grating optical sensor using guided mode," *IEEE J. Quantum Electron.*, vol. 51, no. 1, pp. 1–8, 2014.

[77] T. Sun, *High contrast grating for optical sensing*, Ph.D. dissertation, Univ. of California, Berkeley, 2015.

[78] Y. Takashima, M. Haraguchi, and Y. Naoi, "GaN-based high-contrast grating for refractive index sensor operating in the blue-violet wavelength region," *Sensors*, vol. 20, no. 16, p. 4444, 2020.

[79] T. T. Hoang, T. S. Pham, X. B. Nguyen, H. T. Nguyen, K. Q. Le, and Q. M. Ngo, "High contrast and sensitive near-infrared refractive index sensors based on metal-dielectric-metal plasmonic metasurfaces," *Physica B: Condensed Matter*, vol. 631, p. 413469, 2022.

[80] G. Finco *et al.*, "Guided-mode resonance on pedestal and half-buried high-contrast gratings for biosensing applications," *Nanophotonics*, vol. 10, no. 17, pp. 4289–4296, 2021.

[81] L. Y. Beliaev *et al.*, "Pedestal high-contrast gratings for biosensing," *Nanomaterials*, vol. 12, no. 10, p. 1748, 2022.

[82] M. Marciniak, G. Gębski, M. Dems, and T. Czyszanowski, "Subwavelength high contrast gratings as optical sensing elements," *Sci. Bull. Phys.*, vol. 38, no. 1219, pp. 61–70, 2017. doi: 10.34658/physics.2017.38.61-70.

[83] W. Fang, Y. Huang, X. Duan, K. Liu, J. Fei, and X. Ren, "High-reflectivity high-contrast grating focusing reflector on silicon-on-insulator wafer," *Chin. Phys. B*, vol. 25, no. 11, p. 114213, 2016. doi: 10.1088/1674-1056/25/11/114213.

[84] A. Elrashidi, "Highly sensitive silicon nitride biomedical sensor using plasmonic grating and ZnO layer," *Mater. Res. Express*, vol. 7, no. 7, p. 075001, 2020.

[85] Z. Gharsallah, M. Najjar, B. Suthar, and V. Janyani, "High sensitivity and ultra-compact optical biosensor for detection of UREA concentration," *Optical and Quantum Electronics*, vol. 50, pp. 1–10, 2018.

[86] J. Zhu, X. Wang, Y. Wu, Y. Su, T. Jia, H. Yang, L. Zhang, Y. Qi, and X. Wen, "Plasmonic refractive index sensors based on one- and two-dimensional gold grating on a gold film," *Photon. Sens.*, vol. 10, pp. 375–386, 2020. doi: 10.1007/s13320-020-0581-5.

[87] M. A. Butt, “High sensitivity design for silicon-on-insulator-based asymmetric loop-terminated Mach–Zehnder interferometer,” *Materials*, vol. 18, no. 4, p. 798, 2025. [Online]. Available: https://doi.org/10.3390/ma18040798.

[88] J. González-Colsa, G. Serrera, J. M. Saiz, F. González, F. Moreno, and P. Albella, "On the performance of a tunable grating-based high sensitivity unidirectional plasmonic sensor," *Opt. Express*, vol. 29, no. 9, pp. 13733–13745, 2021. doi: 10.1364/OE.421198.

[89] X. Wang, J. Zhu, Y. Xu, Y. Qi, L. Zhang, H. Yang, and Z. Yi, "A novel plasmonic refractive index sensor based on gold/silicon complementary grating structure," *Chin. Phys. B*, vol. 30, no. 2, p. 024207, 2021. doi: 10.1088/1674-1056/abd9f6.

[90] J. N. Dash and R. Jha, "SPR biosensor based on polymer PCF coated with conducting metal oxide," *IEEE Photon. Technol. Lett.*, vol. 26, no. 6, pp. 595–598, Mar. 2014.

[91] C. Lin and S. Chen, "Theoretical investigation of detection accuracy of surface plasmon resonance sensor with dielectric layer," *Journal of Nanophotonics*, vol. 11, no. 4, pp. 046014-046014, 2017.

[92] A. K. Mishra, S. K. Mishra, and B. D. Gupta, "SPR based fiber optic sensor for refractive index sensing with enhanced detection accuracy and figure of merit in visible region," *Optics Communications*, vol. 344, pp. 86-91, 2015.

[93] B. Raj, P. Kaur, P. Kumar, and S. S. Gill, "Comparative analysis of OFETs materials and devices for sensor applications," Silicon, pp. 1–9, 2022. doi: 10.1007/s12633-022-02110-2.

[94] R. K. Verma and B. D. Gupta, "Surface plasmon resonance-based fiber optic sensor for the IR region using a conducting metal oxide film," *J. Opt. Soc. Am. A*, vol. 27, no. 4, pp. 846–851, 2010.

[95] M.-C. Navarrete, N. Díaz-Herrera, A. González-Cano, and Ó. Esteban, "Surface plasmon resonance in the visible region in sensors based on tapered optical fibers," *Sens. Actuators B*, vol. 190, pp. 881–885, 2014.

[96] N. K. Sharma, M. Rani, and V. Sajal, "Surface plasmon resonance-based fiber optic sensor with double resonance dips," *Sens. Actuators B*, vol. 188, pp. 326–333, 2013.

[97] N. M. Y. Zhang, D. J. J. Hu, P. P. Shum, Z. Wu, K. Li, T. Huang, *et al.*, "Design and analysis of surface plasmon resonance sensor based on high-birefringent microstructured optical fiber," *J. Opt.*, vol. 18, no. 6, p. 065005, 2016.

[98] J. N. Dash and R. Jha, "SPR biosensor based on polymer PCF coated with conducting metal oxide," *IEEE Photonics Technol. Lett.*, vol. 26, no. 6, pp. 595–598, Mar. 2014.

[99] D. Gao, C. Guan, Y. Wen, X. Zhong, and L. Yuan, "Multi-hole fiber-based surface plasmon resonance sensor operated at near-infrared wavelengths," *Opt. Commun.*, vol. 313, pp. 94–98, 2014.

[100] V. Duyne, "Optical biosensors based on plasmonic nanostructures: A review," *Proc. IEEE*, vol. 104, no. 12, pp. 2380–2408, Dec. 2016. doi: 10.1109/JPROC.2016.2624340.

[101] Naresh, V., & Lee, N., "A Review on Biosensors and Recent Development of Nanostructured Materials-Enabled Biosensors," *Sensors*, vol. 21, no. 4, p. 1109, 2021, doi: 10.3390/s21041109.

[102] Y.T. Chen, Y.C. Lee, Y.H. Lai, J.C. Lim, N.T. Huang, C.T. Lin, and J.J. Huang, "Review of Integrated Optical Biosensors for Point-of-Care Applications," *Biosensors*, vol. 10, no. 12, p. 209, 2020, doi: 10.3390/bios10120209.

[103] B. Prabowo, A. Purwidyantri, and K.C. Liu, "Surface plasmon resonance optical sensor: A review on light source technology," *Biosensors*, vol. 8, no. 3, p. 80, 2018. doi: 10.3390/bios8030080.

[104] N. Varnakavi and N. Lee, "A review on biosensors and recent development of nanostructured materials-enabled biosensors," *Sensors*, vol. 21, no. 4, p. 1109, Feb. 2021. doi: 10.3390/s21041109.

[105] S. Mostufa *et al.*, "Advancements and Perspectives in Optical Biosensors," *ACS Omega*, vol. 9, no. 23, pp. 24181–24202, 2024, doi: 10.1021/acsomega.4c01872.

[106] Y. Wang, A. C. Overvig, S. Shrestha, R. Zhang, R. Wang, N. Yu, and L. Dal Negro, "Tunability of indium tin oxide materials for mid-infrared plasmonics applications," *Opt. Mater. Express*, vol. 7, pp. 2727–2739, 2017, doi: 10.1364/OME.7.002727.

[107] D. Gao, J. Ding, and Q. Zhang, "High contrast gratings for biochemical sensing: principles, structures, and applications," Journal of Lightwave Technology, vol. 39, no. 4, pp. 982-995, 2021.

[108] C. W. Cheng and J. K. Chen, "Drilling of copper using a dual-pulse femtosecond laser," *Technologies*, vol. 4, no. 1, p. 7, 2016. doi: 10.3390/technologies4010007.

[109] W. Fang, Y. Huang, X. Duan, K. Liu, J. Fei, and X. Ren, "High-reflectivity high-contrast grating focusing reflector on silicon-on-insulator wafer," *Chinese Physics B*, vol. 25, no. 11, p. 114213, 2016. doi: 10.1088/1674-1056/25/11/114213.

[110] S. Rajput, V. Kaushik, P. Babu, P. Tiwari, A. K. Srivastava, and M. Kumar, "Optical modulation via coupling of distributed semiconductor heterojunctions in a Si-ITO-based subwavelength grating," *Phys. Rev. Appl.*, vol. 15, no. 5, p. 054029, 2021. doi: 10.1103/PhysRevApplied.15.054029.

[111] A. Garg and S. Rai, "Mitigating network adaptation and QoT prediction challenges in WDM networks," *J. Opt. Commun.*, vol. 45, 2023. doi: 10.1515/joc-2023-0324.

[112] M. J. Heck, J. F. Bauters, M. L. Davenport, D. T. Spencer, and J. E. Bowers, "Ultra-low loss waveguide platform and its integration with silicon photonics," *Laser & Photonics Reviews*, vol. 8, no. 5, 2014. doi: 10.1002/lpor.201300183.

[113] P. K. Teotia and R. Kaler, "Multilayer with periodic grating based high performance SPR waveguide sensor," *Optics Communications*, vol. 395, 2017. doi: 10.1016/j.optcom.2016.06.008.

[114] P. K. Teotia and R. Kaler, "1-D grating based SPR biosensor for the detection of lung cancer biomarkers using Vroman effect," *Optics Communications*, vol. 406, 2018. doi: 10.1016/j.optcom.2017.03.079.

[115] Z. Li, B. Xu, L. Liu, J. Xu, C. Chen, C. Gu, and Y. Zhou, "Localized spoof surface plasmons based on closed subwavelength high contrast gratings: concept and microwave-regime realizations," *Scientific Reports*, vol. 6, no. 1, 2016. doi: 10.1038/srep27158.

[116] D. Urbonas, R. F. Mahrt, and T. Stöferle, "Low-loss optical waveguides made with a high-loss material," *Light: Science & Applications*, vol. 10, no. 1, 2021. [Online]. Available: https://doi.org/10.1038/s41377-020-00454-w

[117] W. Fang, X. Fan, H. Niu, X. Zhang, H. Xu, N.-K. Chen, and C. Bai, "Polarization insensitivity filter using 2D subwavelength high contrast gratings," in *Asia Communications and Photonics Conference*, Optical Society

of America, 2018, pp. Su2A–129. [Online]. Available: https://doi.org/10.1109/ACP.2018.8595906

[118] Y. Zhou, V. Karagodsky, B. Pesala, F. G. Sedgwick, and C. J. Chang-Hasnain, "A novel ultra-low loss hollow-core waveguide using subwavelength high-contrast gratings," *Optics Express*, vol. 17, no. 3, 2009. [Online]. Available: https://doi.org/10.1364/OE.17.001508

[119] V. Myroshnychenko, J. Rodríguez-Fernández, I. Pastoriza-Santos, A. M. Funston, C. Novo, P. Mulvaney, L. M. Liz-Marzán, and F. J. G. de Abajo, "Modelling the optical response of gold nanoparticles," *Chemical Society Reviews*, vol. 37, no. 9, 2008. [Online]. Available: https://doi.org/10.1039/b711486a

[120] Y.-W. Lin, T.-H. Chang, T.-H. Her, and H.-Y. Yao, "Thin-film dielectric characterization by bound state in the continuum in high contrast grating," *Optics Express*, vol. 32, no. 20, pp. 36048–36062, 2024.

[121] S. Tang, S. A. Dereshgi, W. Hadibrata, I. Tanriover, and K. Aydin, "Highly efficient light absorption of monolayer graphene by quasi-bound state in the continuum," *Nanomaterials*, vol. 11, no. 2, p. 484, 2021. [Online]. Available: https://doi.org/10.3390/nano11020484

[122] L. Y. Beliaev, S. Kim, B. F. S. Nielsen, M. V. Evensen, et al., "Optical biosensors based on nanostructured silicon high-contrast gratings for myoglobin detection," *ACS Applied Nano Materials*, vol. 6, no. 13, p. 12364, 2023.

[123] P. R. West, S. Ishii, G. V. Naik, N. K. Emani, V. M. Shalaev, and A. Boltasseva, "Searching for better plasmonic materials," *Laser & Photonics Reviews*, vol. 4, no. 6, 2010. [Online]. Available: https://doi.org/10.1002/LPOR.200900055

[124] B. Painam, R. Kaler, and M. Kumar, "Photonic crystal waveguide biochemical sensor for the approximation of chemical components concentrations," *Plasmonics*, 2016. [Online]. Available: https://doi.org/10.1007/s11468-016-0341-z

[125] Y. Al-Qazwini, P. Arasu, and A. Noor, "Numerical investigation of the performance of an SPR-based optical fiber sensor in an aqueous environment using finite-difference time domain," in *Proceedings of the 2011 IEEE 2nd International Conference on Photonics (ICP)*, 2011, pp. 1–4. [Online]. Available: https://doi.org/10.1109/ICP.2011.6106886

[126] E. D. Palik, *Handbook of Optical Constants of Solids*, vol. 3. Academic Press, 1998.

[127] C. Chase, Y. Zhou, and C. J. Chang-Hasnain, “Size effect of high contrast gratings in VCSELs,” *Opt. Express*, vol.17,no.26, pp. 24002–24007, 2009.